

SOLAR ULTRAVIOLET IMAGING TELESCOPE DATA SIMULATOR

A DISSERTATION

*Submitted in partial fulfilment of the
requirements for the award of the degree*

of

MASTER IN TECHNOLOGY

in

SOLID STATE ELECTRONIC MATERIALS

by

AMRITA UNNIKRISHNAN

(16550001)



DEPARTMENT OF PHYSICS

INDIAN INSTITUTE OF TECHNOLOGY ROORKEE

ROORKEE – 247667 (INDIA)

MAY, 2018

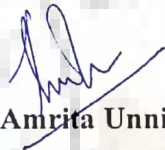
CANDIDATE'S DECLARATION

I hereby declare that the work which is presented in this thesis, entitled, "SOLAR ULTRA VIOLET IMAGING DATA SIMULATOR", submitted in partial fulfillment of the requirement for the award of the degree of Master of Technology in "Solid State Electronic Materials" in Department of Physics, Indian Institute of Technology Roorkee, is an authentic record of my own work carried out during the period from May 2017 to April 2018 under the supervision and guidance of Dr. Anil Kumar Gourishetty, Indian Institute of Technology Roorkee, Prof. A. N. Ramaprakash and Prof. Durgesh Tripathi, Inter-University Centre for Astronomy and Astrophysics.

I also declare that I have not submitted the matter embodied in this report for award of any other degree.

Date: 07.05.2018

Place: Roorkee


(Amrita Unnikrishnan)

CERTIFICATE

This is to certify that the above statement made by the candidate is correct to the best of my knowledge.

Dr. Anil Kumar Gourishetty

Assistant Professor

Department of Physics

Indian Institute of Technology

Roorkee – 247 677



Prof. Durgesh Tripathi

Associate Professor, IUCAA



Prof. A. N. Ramaprakash

Professor, IUCAA

“Equipped with his five senses, man explores the universe around him and calls the adventure Science”

Edwin Hubble





Abstract

Aditya L1 is Indian Space Research Organisation's (ISRO) first space mission to study the Sun. Solar Ultraviolet Imaging Telescope(SUIT), is an imaging instrument on board Aditya L1 which will observe the Sun in the 200-400nm bandwidth. As part of SUIT's on-board intelligence, it tracks a Region Of Interest(ROI) uploaded by the user. The instrument starts tracking the ROI at the stipulated time for a predefined duration, both uploaded by the user. When a solar flare occurs, SUIT localises the location of the flare and tracks it over a period of time. This work proposes algorithms to implement ROI and flare tracking, which can be later implemented on an Field Programmable Gate Array(FPGA) with permissible error margins.

Acknowledgements

I wish to express my gratitude to Prof. A. N. Ramaprakasah and Prof. Durgesh Tripathi for their guidance and constant support extended to me while working on my project. I thank them for permitting me to do my project here in IUCAA and utilise the facilities here. I thank Mr. Mahesh P. Burse, Dr. Sreejith Padinhatteeri, Mr. Aafaq Khan, and Ms Avyarthana Ghosh for their help and support.

I take this opportunity to thank Dr. Anil Kumar Gourishetty, for having reposed confidence in me to take up this project. His constant encouragement has helped me pass through the testing times. I would like to thank my friends in IUCAA and IIT, Roorkee for their support extended to me. Last but not the least I would like to thank my family for standing by me and supporting me in all possible ways within their means.



Contents

Abstract	ii
Acknowledgements	iii
List of Figures	vi
List of Tables	viii
Abbreviations	ix
1 Introduction	1
1.1 SUIT	3
1.2 Construction and Working of SUIT	4
2 Literature Survey	6
2.1 Solar Atmosphere	6
2.1.1 Photosphere	7
2.1.2 Chromosphere	7
2.1.3 Corona	8
2.2 Solar Flares and Coronal Mass Ejections	8
2.3 Differential Rotation	9
2.4 Coordinate Systems	9
2.5 Heliographic Coordinates	10
2.6 Heliocentric Coordinates	11
2.7 Helioprojective Coordinates	11
2.8 Software Implementation	12
2.8.1 hel2arcmin.pro	12
2.8.2 arcmin2hel.pro	13
2.9 Lagrange points: Earth Sun system	13
3 Objective of SUIT Data Simulator	15
3.1 Preparing Test Images	15
3.2 ROI Tracking	16
3.3 Flare Tracking	16
3.4 Challenges	17

4	Implementation	19
4.1	Instruction Set	19
4.2	ROI Tracking	20
4.2.1	Algorithm 1	20
4.2.2	Algorithm 2	21
4.2.3	Algorithm 3	24
4.2.4	Algorithm 4	25
4.2.5	Algorithm 5	26
4.3	Flare Tracking	28
4.3.1	LUT method	29
4.3.2	Flare Cartesian Spherical Coordinate Method	29
5	Results and Discussion	32
5.1	ROI Tracking	32
5.2	ROI Algorithms	34
5.3	Flare Algorithms	36
5.4	Error Calculation	37
5.4.1	ROI Tracking	37
5.4.2	Flare Tracking	39
6	Summary and Conclusion	44
	Bibliography	45

List of Figures

1.1	Aditya L1 Image Courtesy:ISRO [1]	2
1.2	Functional diagram of SUII Image Courtesy:A.Ghosh et al [2]	5
2.1	Layers of the Sun Image Courtesy:ISAS/JAXA	7
2.2	Sun Earth Lagrangian points Image Courtesy:ISRO	14
3.1	Orientation of the Sun with the top of the CCD Image Courtesy: SDO HMI	17
3.2	Projection of a sphere to a 2D plane Image Courtesy: A.Ahmad et al [3]	18
4.1	ROI Tracking: Algorithm 1	22
4.2	ROI Tracking: Algorithm 2	23
4.3	Lookup Table for Algorithm 3	24
4.4	ROI Tracking: Algorithm3	25
4.5	Pixel Shift along latitude-longitude bands Image Courtesy:SDO HMI	26
4.6	Pixel Shift along latitude-longitude bands when there is 40° angle between the Solar North and the top of the CCD Image Courtesy:SDO HMI	27
4.7	ROI Tracking: Algorithm 4	28
4.8	Spherical to cartesian coordinates Conversion	29
4.9	ROI Tracking: Algorithm 5	30
4.10	Flare Tracking: Algorithm 5	31
5.1	ROI tracking about [40,30] and theta = 0° for 24 hours	33
5.2	ROI tracking about [-50,-40] and theta = 30° for 24 hours	34
5.3	ROI tracking about [-50,-40] and theta = -30° for 24 hours	35
5.4	Comparative study of the ROI tracking algorithms	37
5.5	Study of the pixel position when longitude is -89° over a period of 23 hours	38
5.6	Study of the pixel position when longitude is -45° over a period of 23 hours	39
5.7	Study of the pixel position when longitude is -89° over a period of 23 hours	40
5.8	Study of the pixel position when longitude is 89° over a period of 23 hours	41

5.9 Study of deviation in pixels from ideal case scenario when longitude= -89° over a period of time 42

5.10 Study of deviation in pixels from ideal case scenario when longitude= -45° over a period of time 42

5.11 Study of deviation in pixels from ideal case scenario when longitude= 45° over a period of time 43

5.12 Study of deviation in pixels from ideal case scenario when longitude= 89° over a period of time 43



List of Tables

2.1 FITS Header parameters in this document. 10



Abbreviations



ISRO	Indian Space Research Organisation
VELC	Visible Emission Line Coronagraph
SUIT	Solar Ultraviolet Imaging Telescope
HEL1OS	the High Energy L1 Orbiting Spectrometer
SoLEX	Soft X-ray Low Energy X-ray Spectrometer
PAPA	Plasma Analyzer Package for Aditya
ASPEX	Aditya Solarwind and Particle Experiment
IIA	Indian Institute of Astrophysics
IUCAA	Inter-University Centre for Astronomy and Astrophysics
PRL	Physical Research Laboratory
ISAC	ISRO Satellite Centre
LEOS	Laboratory for Electro-optic Systems
POC	Payload Operation Center
LUT	Look Up Table
ROI	Region of Interest
CCD	Charge Coupled Device
FPGA	Field Programmable Gate Array

Chapter 1

Introduction

Aditya L1 is India's first solar mission planned to be launched in 2020 during the beginning of the next solar cycle. It will be launched at the Lagrange 1(L1) point of the Sun-Earth system. Discussed later in section 2.9, a satellite in L1 would give it an unobstructed and continuous view of the Sun.

Different layers of the Solar atmosphere radiate in different wavelength bands due to the different temperature zones in its interior and atmosphere. As the harmful ultra]violet (UV) and X rays are absorbed by the earth's atmosphere, studying Sun from space would help us to study it across wavelengths, understand the dynamics and physics of the solar atmosphere.

Aditya L1 will have seven payloads namely, the Visible Emission Line Coronagraph (VELC), the Solar Ultraviolet Imaging Telescope (SUIT), the High Energy L1 Orbiting Spectrometer(HEL1OS), the Soft X-ray Low Energy X-ray Spectrometer (SoLEX), the Plasma Analyzer Package for Aditya (PAPA), Aditya Solarwind and Particle Experiment (ASPEX) and a Magnetometer. The scope and objective of each payload are discussed below [1]:

1. **Visible Emission Line Coronagraph (VELC):** Developed at the Indian Institute of Astrophysics (IIA) it proposes to study the diagnostic parameters

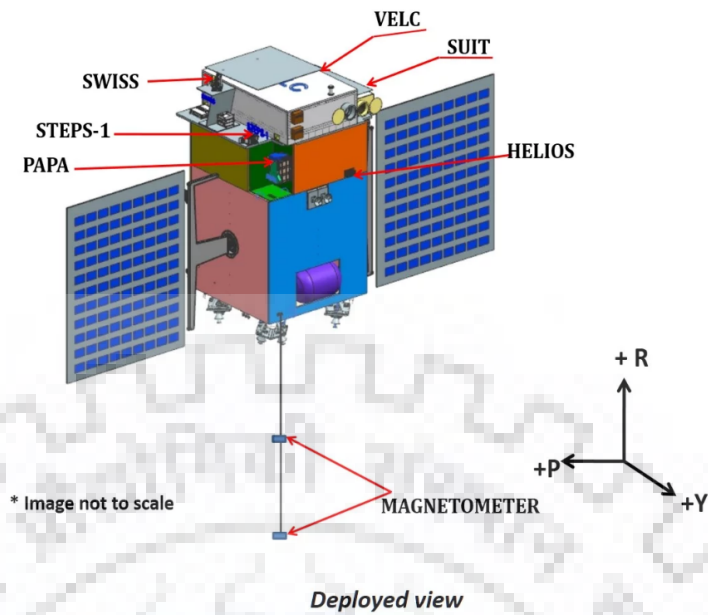


FIGURE 1.1: Aditya L1
Image Courtesy:ISRO [1]

of solar corona and dynamics and origin of Coronal Mass Ejections. It will also study the magnetic field measurement of the solar corona.

2. **Solar Ultraviolet Imaging Telescope (SUIT):** This instrument will image the spatially resolved Solar photosphere and chromosphere in near Ultraviolet (200-400 nm) and measure solar irradiance variations. It is being developed at Inter-University Centre for Astronomy & Astrophysics (IUCAA)
3. **Aditya Solar wind Particle Experiment (ASPEX):** Physical Research Laboratory (PRL) is developing ASPEX to study the variation of solar wind properties as well as its distribution and spectral characteristics
4. **Plasma Analyser Package for Aditya (PAPA):** PAPA aims to understand the composition of solar wind and its energy distribution. It is being developed at Space Physics Laboratory (SPL), VSSC
5. **Solar Low Energy X-ray Spectrometer (SoLEXS):** SoLEX would monitor the X-ray flares for studying the heating mechanism of the solar corona. It is being developed at ISRO Satellite Centre (ISAC)

6. **High Energy L1 Orbiting X-ray Spectrometer (HEL1OS):** To observe the dynamic events in the solar corona and provide an estimate of the energy used to accelerate the particles during the eruptive events, ISRO Satellite Centre (ISAC) and Udaipur Solar Observatory (USO), PRL are developing HEL1OS.
7. **Magnetometer:** A magnetometer to measure the magnitude and nature of the Interplanetary Magnetic Field is being developed at Laboratory for Electro-optic Systems (LEOS) and ISAC.

1.1 SUIT

VELC observes the solar corona from 1.05–3.0 solar radius, providing information on the dynamics of the lower solar corona. But it would not provide information on activities happening at the Solar disk. SoLEX and HEL1OS observe the Sun as a Star and hence do not have any spatial information regarding solar activity.

To understand solar activities which are later discussed in section 2.2, we need to study the regions from where they initiated and how they evolve. Hence an imager called the Solar Ultraviolet Imaging Telescope (SUIT) was proposed to help us to study interplay and interconnection between transition region and corona. Located at L1, SUIT would observe the Sun in near ultraviolet wavelength range of 200-400nm in eleven different wavelength bands, which would otherwise have been attenuated by Earth's atmosphere. This will provide near simultaneous observations of the Sun from the photosphere, chromosphere, and lower transition region. Hence, combining the observations from VELC, SoLEX, HEL1OS, and SUIT we can study all the layers of the solar atmosphere.

Of the total Solar irradiance, only 8% is emitted in UV. However, more than 60% of the solar variability takes place in the UV region. These fluctuations are highly sensitive to the temperature fluctuations and poorly understood. SUIT would throw light on this strange variation in UV solar flux.

The science objectives of SUIT payload are[2]:

- a) Coupling and Dynamics of the Solar Atmosphere: What are the processes through which the energy is channelized and transferred from the photosphere to the chromosphere and then to the corona?
- b) Prominence Studies from SUIT: What are the mechanisms responsible for stability, dynamics and eruption of solar prominences?
- c) Initiation of CMEs and Space Weather: What are the kinematics of erupting prominences during the early phase?
- d) Sun-Climate studies with SUIT: How strongly does the solar irradiance of relevance for the Earth's climate vary?

1.2 Construction and Working of SUIT

SUIT consists of a RitcheyChrtien telescope, a set of science filters and a CCD detector to capture high-resolution images of the solar disk in UV region between 200-400 nm. The instrument has two main sub-units: the optical bench and the payload electronics box. The former consists of mirrors, focal plane assembly, filter wheel mechanism, shutter mechanism, entrance baffles and a thermal filter.

The entrance baffle allows collimated Sun rays and prevents reflections from surrounding components into the payload cavity. Entrance baffle assembly consists of entrance baffle and the door assembly.

As discussed in the previous section, the UV region comprises only about 8% of the total solar flux. To prevent heating of the components in the payload and saturation of the detector due to excess flux most of the incoming flux has to be cut down. The thermal filter at the opening of the payload cuts out the radiation from the visible and IR bands and allows only UV band to pass through.

As shown in figure 1.2 the incident photons passes through the primary and secondary hyperbolic mirrors of the telescope. The mirrors are cut out such that the reflection from the primary mirror falls on the secondary mirror. The photons then

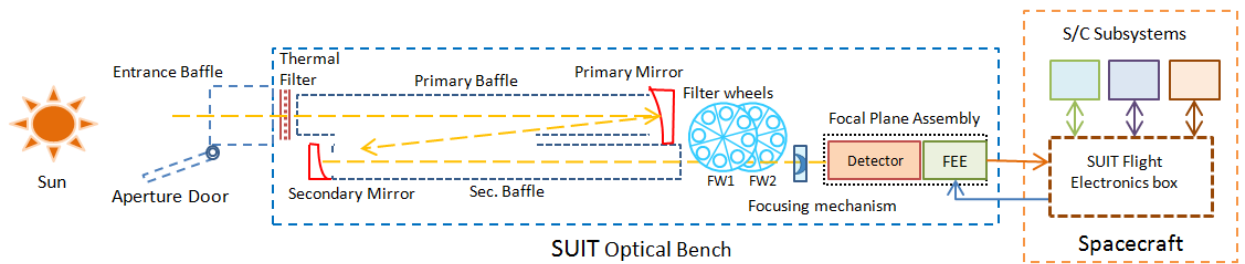


FIGURE 1.2: Functional diagram of SUIT
Image Courtesy: A. Ghosh et al [2]

pass through a combination of filters with the help of the filter wheels. The beam is then focused on to the CCD detector by the focusing mechanism. The focusing mechanism is nothing but a field corrector lens. A shutter mechanism is provided before the filter wheels to prevent radiation falling on the detector. The CCD is 4096×4096 pixels detector with a field-of-view (FoV) of 0.6 along each axis. It is divided into 25 equally spaced symmetric blocks.

SUIT has total 11 science filters which include 8 narrow-band and 3 broadband filters that will be mounted on two independent filter wheels. Each filter wheel has 8 slots. Of the 16 available slots, 11 are the science filters. Of the remaining five slots one is in a closed position takes dark frames and the remaining are neutral density filters. The neutral density filters also help in cutting down the flux. Combinations of different filters allow only desirable bands of wavelength to pass through. Optical alignment of all the components has to be maintained both during operational and non-operational modes.

Chapter 2

Literature Survey

The Sun is a hot ball of gases located at the center of the solar system. With a diameter of about 1.4 million kilometers (109 times of that of Earth) and a mass of 1.989×10^{30} kg, the Sun is about 4.603 billion years old. Located approximately 150 million kilometers away from Earth, Sun is Earth's primary source of energy. It is this energy which supports life on Earth and controls its climate. Hence, it is important for us to understand its structure and functioning.

2.1 Solar Atmosphere¹

The solar interior consists of the core, radiative zone and the convection zone. Solar atmosphere consists of the Corona, Photosphere and Chromosphere.

The core is where all the energy for solar activity is created. High pressure due to gravity and the high temperature keeps the gases in ionised form. The loose hydrogen nuclei and proton helps in nuclear reactions which results in generating huge amounts of energy. The radiative zone ranges from 0.25 to 0.7 solar radii. Here energy transfer happens in the form of gamma ray photons. They collide and then absorbed by other gas molecules and remitted as photons of the same wavelength till they reach the photosphere. From 0.7 solar radii and beyond the

¹<https://www.astro.cf.ac.uk/observatory/solarobservatory/background/?page=interior>

convection region begins. Hot gas rises up to be replaced by cooler gas. Though transfer of energy is faster in convective zone compared to radiative zone, a photon still takes a long time to reach the photosphere.

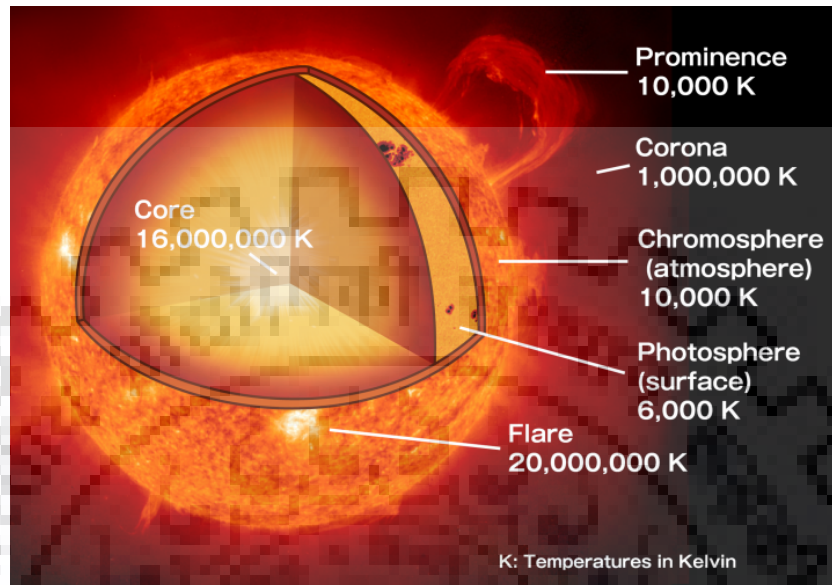


FIGURE 2.1: Layers of the Sun
Image Courtesy: ISAS/JAXA

2.1.1 Photosphere

The photosphere is the lowest layer of the solar atmosphere. It is a 400km wide layer of gases. It is opaque to visible light and hence can be easily viewed. Here temperature varies from 6500 K at the bottom to 4000 K at the top. Most of the photosphere is covered by granulation. Granulation at the photosphere helps in transporting heat from lower layers to the surface.

2.1.2 Chromosphere

The chromosphere is the middle layer, sandwiched between the photosphere and the solar surface. It ranges from 400 km to 2100 km from the photosphere. It is transparent to visible light, and cannot be seen due to the brightness of the photosphere. Temperature in this region ranges from 4400K to 25000K at the top. That is it gets hotter as one moves away from the center.

2.1.3 Corona

The outermost layer of the Sun is called its Corona. It starts at about 2100 km from the photosphere. Its temperature varies in the range of 500, 000 K. Though the corona has a much higher temperature than the surface of the Sun it is millions of times less denser than the surface making it less brighter than its surrounding. This results in the corona getting hidden by the bright light from the Sun. Hence one cannot see it with naked eyes, but it can be viewed using a coronagraph. During total solar eclipse the corona can be seen with naked eyes.

2.2 Solar Flares and Coronal Mass Ejections

Both Solar Flares and Coronal mass ejections are massive bursts of mass and energy caused by the disentanglement of entangled solar magnetic fields. Bursts of energy coupled with ejection of plasma is referred to as Coronal Mass Ejection(CME). It travels at a speed of millions of kilometre an hour and takes about 2 to 3 days to reach Earth.

Flares can disturb the Earth's atmosphere causing blackouts in the communication networks. CME's pushes charged particles into the Earth's space disturbing its magnetic fields. Current due to the magnetic fields pushes the charged particles near the poles where they react with Nitrogen and Oxygen creating aurora lights. Like flares, CME's can disrupt the communication and electrical networks.

Sun spots are cooler (around 3000 K) and darker regions(in comparison to their surrounding bright region) on the Photosphere(around 5000K). They spread across large areas in diameter and appear in regions of intense magnetic fields.The energy from these magnetic fields are ejected in the form of solar flares or CMEs.

2.3 Differential Rotation

The Sun is not a rigid body instead it spins along its latitudes such that it is fastest at the equator and slowest at the poles. A sunspot at the equator would take 25 days to complete one rotation while a sunspot at the poles would take 35 days to complete one rotation. The relation between the speed of rotation and the latitude is given by the below relation:

$$\omega = A + B\sin^2(\phi) + C\sin^4(\phi) [4] \quad (2.1)$$

here ω is the angular velocity in degrees per day and ϕ is the latitude in degrees. The constants A, B, C are defined as:

$$A = 14.713 \pm 0.0491^\circ / \text{d}$$

$$B = -2.396 \pm 0.188^\circ / \text{d}$$

$$C = -1.787 \pm 0.253^\circ / \text{d}$$

2.4 Coordinate Systems

A coordinate system for interplanetary space is in common use among the astronomical community. In case of solar physics and solar instrumentation view the sun in different perspectives giving rise to a need for a common coordinate system.

The coordinate system for solar data has to be three dimensional to take into account activities in the corona or anywhere else on the surface of the Sun. Given the gaseous nature of Sun it is difficult to fix a point of reference. To observe a particular region on the Sun one needs to take into account its differential rotation. Also the observations are dependant on the position of the observer. The Sun appears about 1% larger in size from the L1 point as to compared to when observed from Earth.

This implies the data obtained from SOHO at L1 will not be in sync with that obtained from SDO at low earth orbit. W T Thompson in his paper on the solar

coordinate system discusses the various possible coordinate systems for Solar data and FITS headers which are closely related to World coordinate System (WCS). This helps in linking solar data from different sources.

The below FITS headers have been used in the algorithms proposed in this work²

FITS Header	Description
CRPIX1	Central Pixel of the CCD about X axis
CRPIX2	Central Pixel of the CCD about Y axis
NAXIS1	Number of columns
NAXIS2	Number of rows
CDELTA1	Plate Scale
RSUN_OBS	Angular radius of the Sun in arc seconds

TABLE 2.1: FITS Header parameters in this document.

2.5 Heliographic Coordinates

In heliographic coordinate system, a feature on the Sun is described in terms of its latitude, longitude and its distance from the center of the Sun (in case of three dimension). The axis of rotation is taken as described by Carrington (1863). Based on the works of Seidelmann et al 2002 the angle of ascension is taken as α_0 as 286.13 and angle of declination is taken as δ_0 as 63.87 degrees. The heliographic coordinates is further classified into Stonyhurst and Carrington based on the definition of longitude. The axis of rotation in both the cases remain the same. The latitude and longitude are given in degrees.

In Stonyhurst system, the point of intersection of the equator and the central meridian (as seen from the Earth) is taken as the origin. Hence while the coordinate system is fixed with respect to the Earth and the Sun rotates below it.

Carrington coordinate system considers the sidereal rotation of the Sun, which is about 25.38 days. When the prime meridian on the Sun coincides with the central

²<https://www.astro.cf.ac.uk/observatory/solarobservatory/background/?page=interior>

meridian while observing from the Earth, it is considered a Carrington rotation. 1 Carrington rotation is about 27.21 to 27.34 days, depending on Earth's position.

Carrington and Stonyhurst coordinate systems are related by the relation $\phi_C = \phi + L_0$. ϕ_C is the Carrington longitude and ϕ is the Stonyhurst longitude. L_0 is a scalar which is time dependent

2.6 Heliocentric Coordinates

In the right handed heliocentric coordinate system, depends on the position of the observer. Therefore, a feature on the Sun when viewed from space and from Earth at the same time have different coordinates in this system. It can be further sub divided into heliocentric Cartesian coordinates system and heliocentric radial coordinates.

The heliocentric cartesian coordinate system has (x, y, z) axes perpendicular to each other. The z axis is defined along the direction from the Sun to the observer while y is defined along the solar north. While the z axis in the heliocentric cartesian and helio radial coordinates are same, ρ gives the radial distance from the z axis and ψ gives the position angle in anti clockwise direction.

2.7 Helioprojective Coordinates

Helioprojective coordinate system is a left handed system. Like helio centric coordinates, helioprojective coordinates are observer dependant, but the distances are measured in terms of angles. The disk center is taken as the origin without correcting for the time taken for the light to travel or aberrations. It can be further sub divided into helioprojective Cartesian coordinates system and heliocentric radial coordinates. In helioprojective Cartesian coordinates, θ_x and θ_y are taken as longitude and latitude respectively. They can be approximated to heliocentric cartesian coordinates by the below relation:

$$x = D_o \left[\frac{\pi}{180} \right] \theta_x \quad (2.2)$$

$$y = D_o \left[\frac{\pi}{180} \right] \theta_y \quad (2.3)$$

D_o is the distance between the Sun and the observer.

Similarly helioprojective radial coordinates ρ and δ are given by

$$\rho = D_o \left[\frac{\pi}{180} \right] \theta_x \quad (2.4)$$

$$\delta = D_o \left[\frac{\pi}{180} \right] \theta_y \quad (2.5)$$

2.8 Software Implementation

The SolarSoft is a collection of software libraries, data bases, and system utilities which provides an environment for programming and analysing data in Solar Physics. The SolarSoftWare (SSW) system is built from Yohkoh, SOHO, SDAC and Astronomy libraries. Though it is primarily an IDL based system, it supports executables from other languages. It provides a common ground for exchanging data and its analysis for both users and among the instruments.

2.8.1 hel2arcmin.pro

This function converts position in heliographic coordinates to arcmin (relative to the Sun's center) taking into account the p and b0 angle. The p and b0 angles can either be entered explicitly or if the date is given it can be calculated. In case date is not provided the default date is taken as the current date. The output is in arcminutes with respect to the Solar center.

2.8.2 arcmin2hel.pro

This function converts position in arcmin (relative to the Sun's center) to its heliographic coordinates taking into account the p and b0 angle. The p and b0 angles can either be entered explicitly or if the date is given it can be calculated. The default date is the current date. The output is in degrees with respect to the Solar center.

2.9 Lagrange points: Earth Sun system

For two heavenly bodies, its Lagrange point is a location in space where the effect of their gravitational forces equals the centrifugal force felt by a much smaller third body[5]. This creates a point of equilibrium where a spacecraft may be launched to take observations. The Earth Sun system has five Lagrangian points as shown in figure 2.2 .

L1 point is about 1.5 million kilometers away from Earth and gives an uninterrupted view of the Sun. Solar and Heliospheric Observatory (SOHO) and the Deep Space Climate Observatory are placed at L1. L2 is also about 1.5 million kilometers away from the Earth but is in direction opposite to L1. L3 lies on the Earth's orbit and it lies behind the Sun. L4 and L5 points lie along Earth's orbit at an angle 60 degrees and are stable points compared to L1,L2, and L3. Their stability attracts dust and asteroids to settle in these regions.

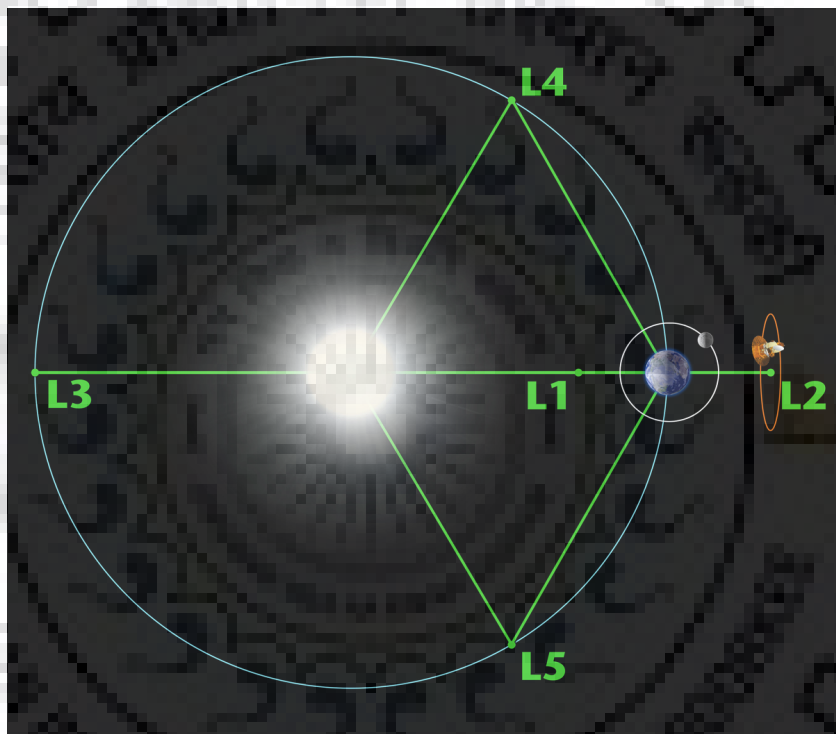


FIGURE 2.2: Sun Earth Lagrangian points
Image Courtesy:ISRO

Chapter 3

Objective of SUIE Data Simulator

This chapter discusses the objective and motivation of the SUIE data simulator. The objective of the SUIE Data Simulator is to simulate the working of SUIE as it would do at the L1 point. ROI tracking and flare tracking the key features of SUIE, are planned to be implemented on an FPGA. The idea of the SUIE data simulator is to re-create the working of SUIE using IDL, find the best possible approach to implement the onboard tasks expected to be performed by SUIE. The approach is tested on all possible scenarios and proved to be effective within permissible error threshold.

3.1 Preparing Test Images

SUIE observes the Sun in the wavelengths between 200 to 400 nm. It uses 11 filters which include 8 narrow band filters and 3 broadband filters in the ultraviolet wavelengths. The images from SUIE are expected to be of size 4096×4096 pixels with a plate scale of 0.7 arc seconds. Using data from previous solar missions, test images are prepared as specified in [2].

3.2 ROI Tracking

One of the key features of SUIT is ROI tracking. The user would want to observe a certain region of solar activity on the Sun for a particular duration. He/She would provide heliographic co-ordinates of the mid point of the region of interest(ROI), the time to start tracking and the duration of time to track the region.

At the given start time, SUIT would enter into the ROI mode. It would calculate the mid point of the ROI and convert it to pixels. The region around the mid point is expanded symmetrically to the size of the ROI. SUIT would then observe this region for the duration of time given by the user. Due to differential rotation of the Sun as discussed in section 2.3, the feature would move horizontally and vertically based on its latitude and the angle between the solar North and the top of the CCD.

In certain circumstances, the payload is occupied with some other activity at the start time of the ROI mode and will not enter the ROI mode at the scheduled time. When the payload is ready to enter the ROI mode, the region would have drifted due to the differential rotation of the Sun. SUIT would then take into account the shift in longitude, calculate the new pixel co-ordinates of the ROI and track it for the remaining duration of time.

3.3 Flare Tracking

Another key feature of SUIT is to track flares and solar prominences. When a flare occurs on the solar disk there is a surge in X ray flux which is detected by SOLEX and HELIOS. SUIT would then receive a flare trigger from SOLEX, HELIOS or a self trigger when a flare is detected.

When SUIT receives one of these triggers it localises the location of the flare and tracks it for a certain period of time (say, two hours). As the feature would shift due to the differential rotation of the Sun SUIT would also shift the range of

pixels it observes accordingly. While the inputs are heliographic co-ordinates and outputs are pixel co-ordinates in ROI tracking, in flare tracking both input and output are pixel co-ordinates.

3.4 Challenges

Earth-Sun L1 point is a halo orbit and the satellite would be revolving around this point. In this case, the pitch angle, roll angle and the yaw angle come into play. As shown in figure 3.1 the solar disk may not fall at the center of the CCD.

While performing ROI and flare tracking, one must take into account the position of the Sun's center pixels, the position of the satellite during observation and the angle that the solar north makes with the top of the CCD.

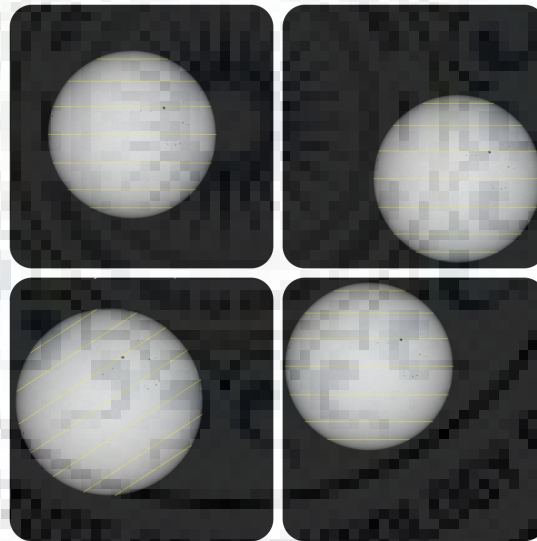


FIGURE 3.1: Orientation of the Sun with the top of the CCD
Image Courtesy: SDO HMI

As discussed in [6] we must study the Sun in three dimensional view to understand solar phenomena from the Sun's interior to the corona. In figure 3.2, a spherical object S_0 of radius R_0 with center at A with coordinates (r_0, θ_0, Φ_0) is in the 3D frame. The outer periphery of S_0 visible to the camera is the circle C_s , which is a circle formed by the contact of the tangential cone Q from O to S_0 . The visible periphery C_s is a circle in 3D frame which forms the base of the cone Q and has a

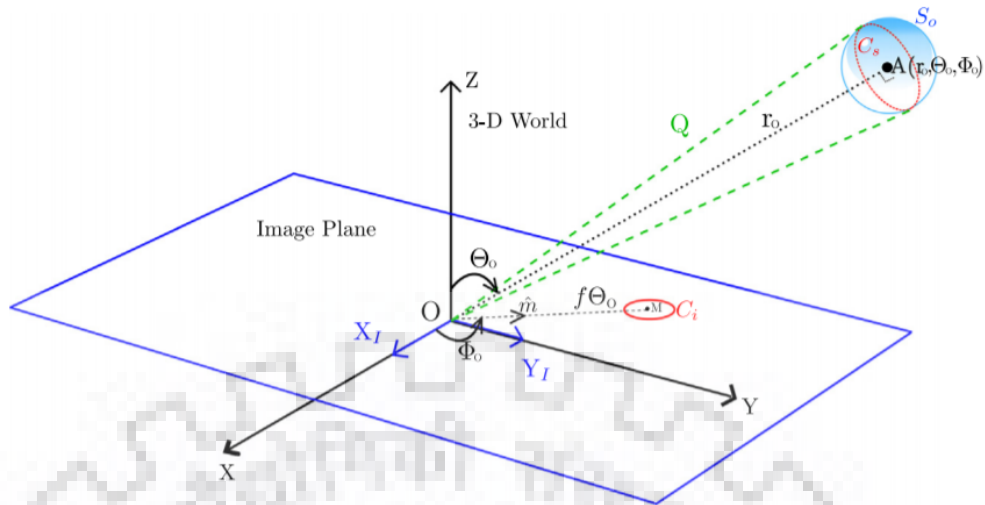


FIGURE 3.2: Projection of a sphere to a 2D plane
Image Courtesy: A.Ahmad et al [3]

radius R_1 ($R_1 < R_0$). Each point on C_s is projected onto the image plane forming a curve C_i . As it can be observed, C_i does not capture all the features of S_0 . The features at the limbs carry more information in fewer pixels compared to the pixels at the center. Hence, the method used for ROI or flare tracking must consider the effects of projection along with other parameters discussed earlier.

A version of SUIT data simulator would also be used on the ground to simulate the working of SUIT at the payload operation center. The user at the ground gets a feel of what to expect from the data coming from the next day. This helps him/her to upload the ROI co-ordinates for the next day. Once the user selects the ROI, he/she uplinks the heliographic coordinates of the center of ROI, the time at which the ROI tracking has to start and the duration for which the ROI is to be tracked. The ground version of SUIT data simulator can also be used to verify the downlinked data.

Chapter 4

Implementation

4.1 Instruction Set

Communication between the ground user and the satellite happens through 32 bit commands. Each command has an 8 bit identifier and other 24 bits are used for the data associated with a command. The commands are classified as :

1. Calculation commands: These commands are for addition, subtraction, increment/decrements, calculating the peak/median etc
2. Action commands: Commands to operate the shutter, CCD, focusing mechanism, detector, filter wheels etc fall under action commands.
3. Check commands: These commands are used to check parameters such as temperature , flag registers etc.
4. Set commands: These commands set parameters or the flag registers
5. General commands: Commands to start, stop or halt an operation fall under general commands.
6. Direct commands : To update any parameter or upload a value direct commands are used.

7. ROI commands: Commands to update ROI table information
8. Update commands: These commands are used to update the program or to update table information.
9. Detector electronics commands: These commands are used to communicate with the detector electronics.
10. Conditional Commands: A certain set of instructions are executed only if its prerequisites are met. Conditional commands checks if the prerequisites are satisfied or not.
11. Data Operations: Instruction for data to travel from CCD to BDH or to choose the mode of CCD operation are the Data operations commands.

4.2 ROI Tracking

As discussed in section 3.2, ROI tracking involves the conversion of heliographic coordinates to pixel units. The approach to tracking the ROI has to be easy to implement and within the permissible errors. This work discusses five different approaches for ROI tracking in the following sections.

4.2.1 Algorithm 1

The first approach towards implementing ROI tracking can be done using `hel2arcmin.pro` which was discussed in section 2.8.1. We know that 1 pixel on the SUIT CCD corresponds to 0.7 arc seconds on the solar disk. We also know the pixel coordinates of the Sun's center. Using this information we can calculate the pixel coordinates for the input heliographic coordinates using the below relation:

$$temp = hel2arcmin(l, b, p = 0, b0 = 0) * 60 * pixelFactor \quad (4.1)$$

$$x = temp[0] + xC \quad (4.2)$$

$$y = temp[1] + yC \quad (4.3)$$

where:

l= heliographic latitude in degrees

b= heliographic longitude in degrees

pixelFactor =1/0.7 .It is the plate scale of the CCD

[xC,yC] = pixel values of the Sun's center

For ROI tracking, the center coordinates of the ROI are taken as inputs. After calculating the pixel values of the central coordinates the region around the point is expanded symmetrically to the size of the ROI. After time 't', calculate the shift in longitude using the formula 2.1 for time 't' and re calculate the pixel coordinates for the 'new' heliographic coordinates. Fig 4.1 explains the flow of logic in executing Algorithm 1. This algorithm has high accuracy and in this study is used as a reference to compare and study the other algorithms that are proposed for ROI tracking.

hel2arcmin.pro uses trigonometric functions like sine, cosine and arctan which are difficult to implement on the FPGA. Hence, it can be used by a user on ground to upload data for the next day.

4.2.2 Algorithm 2

This algorithm approximates the projection of the solar disk as a circle and uses the equation of a circle to calculate the pixel coordinates. It uses a scaling factor 's' to convert latitude or longitude degrees to pixel units. The constant parameters like the scaling factor, angular size of the Sun, radius of the Sun and the Sun's centre in pixels needed for calculation are pre calculated and stored in a look up table. They are fetched as and when required during the computation process.

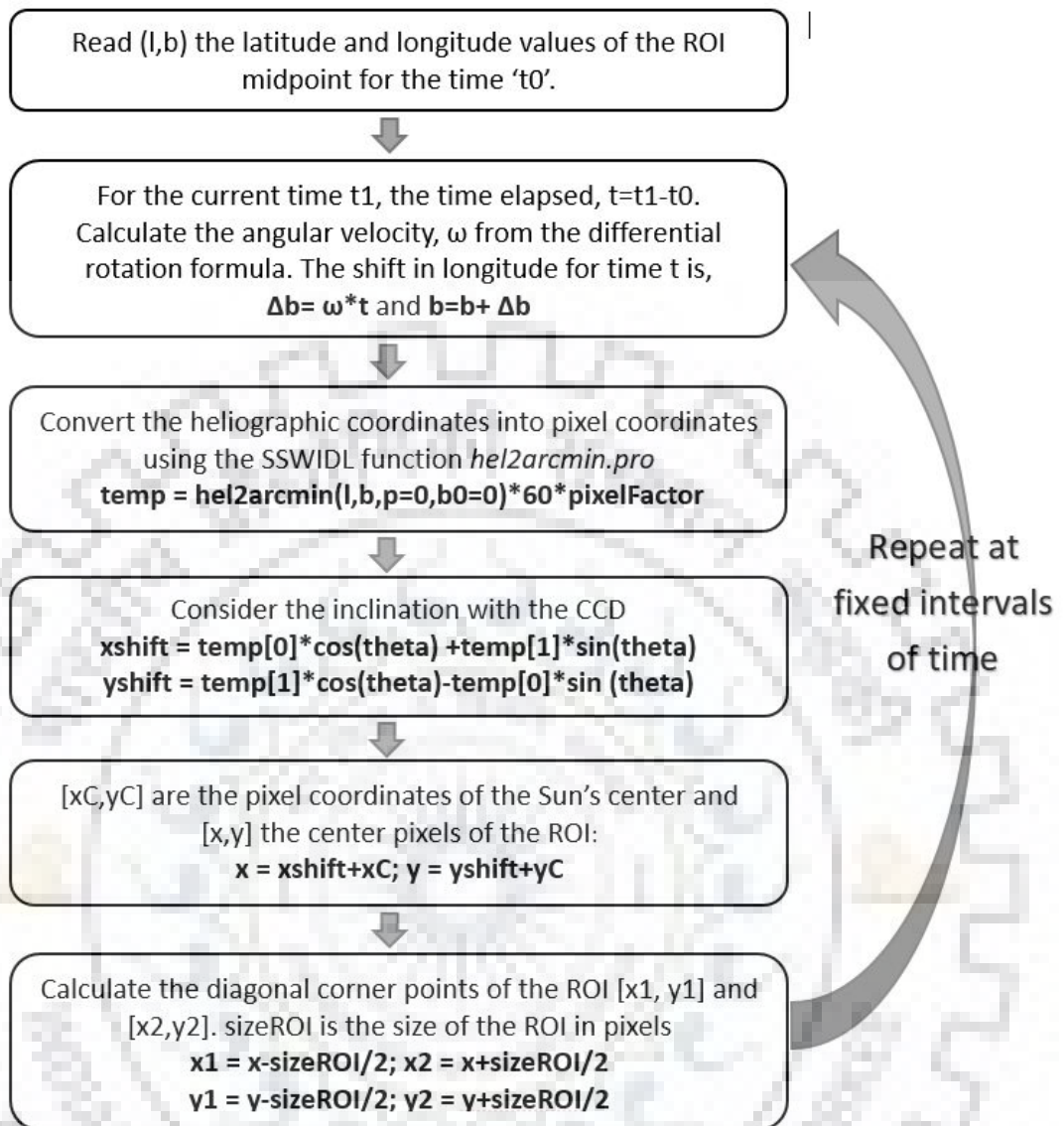


FIGURE 4.1: ROI Tracking: Algorithm 1

The scaling factor s is calculated using the below formula:

$$s = a * pixelFactor * 3600/180 \quad (4.4)$$

where a = angular size of the Sun in degrees

$pixelFactor = 1/0.7$. It is the plate scale of the CCD

The radius of the Sun, R is calculated using:

$$R = 90 * s \quad (4.5)$$

where s , the scaling factor calculated from equation 4.4 The calculations to find the x and y pixel coordinates are explained in figure 4.2.

This algorithm works best at the equator and lower latitudes. The error becomes significant at the poles. This algorithm also uses sine function and square root for calculation. The sine function can be implemented using two methods. The first being storing the sine values in a lookup table (similar to how the constants are stored) and fetching the value as and when required. The second method would be to use Taylor series expansion to implement the sine function.

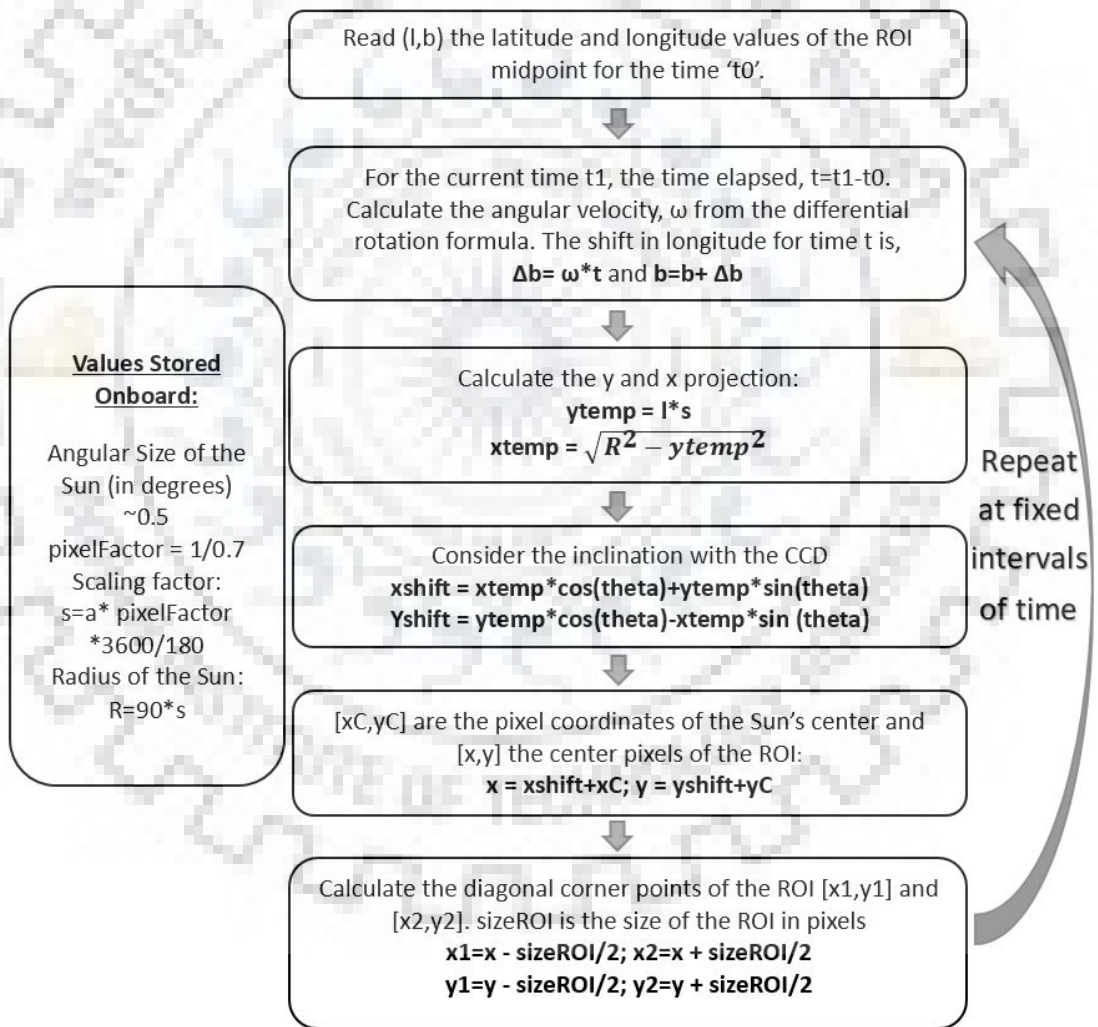


FIGURE 4.2: ROI Tracking: Algorithm 2

4.2.3 Algorithm 3

The third approach proposes to pre-calculate the pixel shifts and store the results in a look up table. The look up table(LUT) will contain the shift in pixels in both x and y directions. As discussed in section 2.8.1, the hel2arcmin.pro function and formula 2.1 can be used to calculate the shift in periodic intervals of time(say fifteen minutes or half an hour). The shift for the entire range of latitudes from -90 to +90 and longitudes from -90 to +90 can be calculated on ground and uploaded.

The angular inclination of the image with respect to the top of the CCD can also be included so that there is no need for calculation to be done on board.

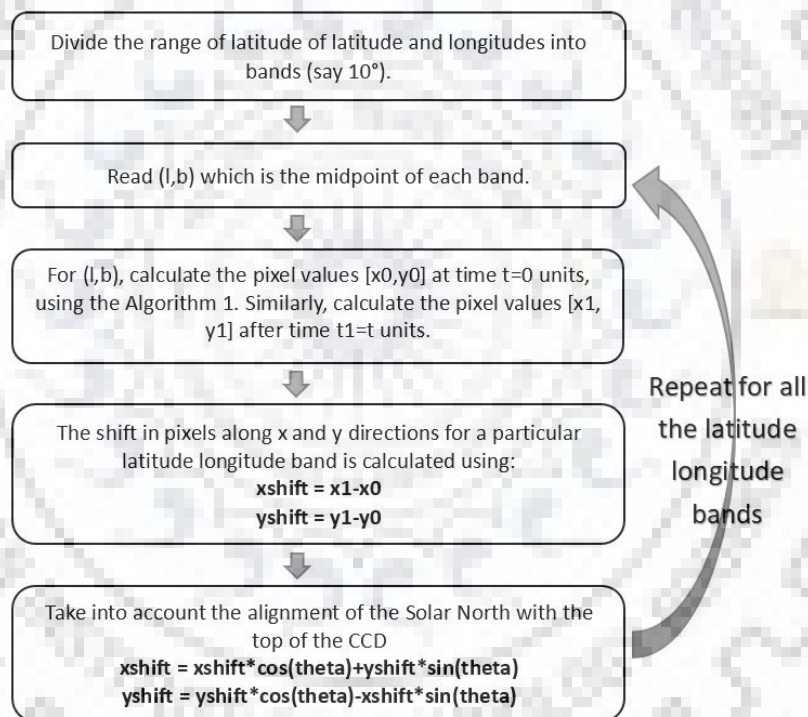


FIGURE 4.3: Lookup Table for Algorithm 3

Figure 4.5 is the superposition of the look up table on the Solar disk when the Solar North is perfectly aligned with the top of the CCD. One can observe that the maximum shift in pixels occurs at the centre while there is a small shift at the limb. As the solar disk is perfectly aligned there is no vertical shift. In figure 4.6 where the solar disk is at angle of 40° with the solar north, there is shift in both

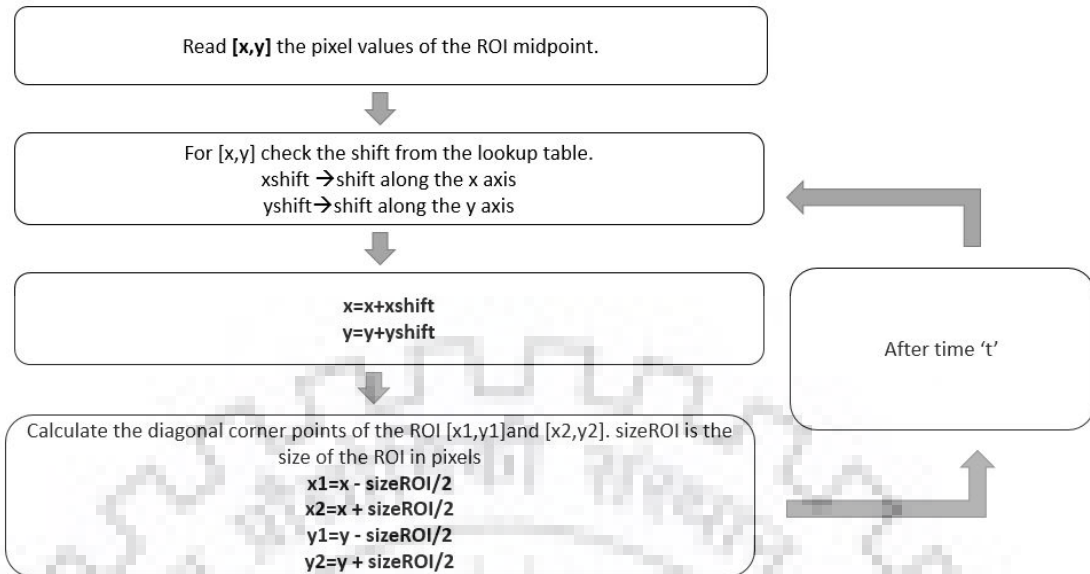


FIGURE 4.4: ROI Tracking: Algorithm3

x and y directions. In both cases, for pixels outside the Solar disk the shift is 0 pixels.

4.2.4 Algorithm 4

The latitude band from 0 to 10 degrees correspond to about 230 pixels and the band from 80 to 90 degrees translate to about 20 pixels. In other words, due to projection 230 pixels in the equatorial region correspond to about 10 degrees while at the polar region 20 pixels translate to 10 degrees. Algorithm 4 calculates bands in terms of pixels. As discussed in section 2.8.2 `arcmin2hel.pro` from SS-WIDL converts pixel coordinates to heliographic coordinates, the inverse function of `hel2arcmin.pro`. The range of pixel values over which the solar disk falls is calculated using `arcmin2hel.pro`.

As described in figure 4.7, for a predefined step size say 256 pixels, we divide the range of pixels into bands of the step size both horizontally and vertically. Using formula 2.1 on the mid point of each band, we can calculate the pixel shift in both vertical and horizontal directions. As described in figure 4.4, on board the shift in pixels happens according to the corresponding value in the look up table. The

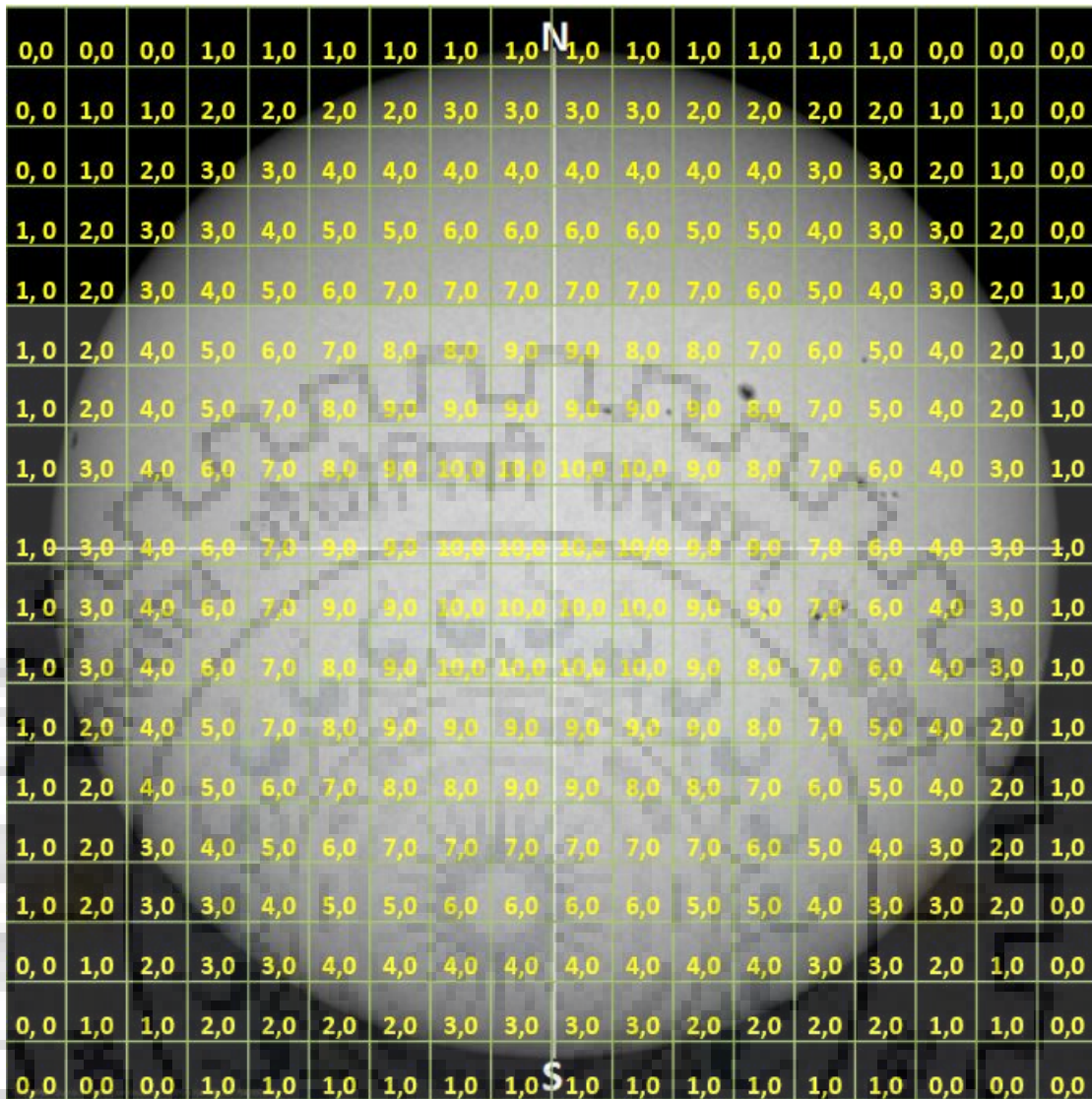


FIGURE 4.5: Pixel Shift along latitude-longitude bands
Image Courtesy:SDO HMI

mode of execution is similar to that of algorithm 3. It differs from algorithm 3 in the way the LUT is developed.

4.2.5 Algorithm 5

Algorithm 5, uses spherical to cartesian conversion formula. Given the solar radius in terms of pixels and latitude-longitude values one can easily convert the input heliographic coordinates to cartesian coordinates as illustrated in the figure 4.8.

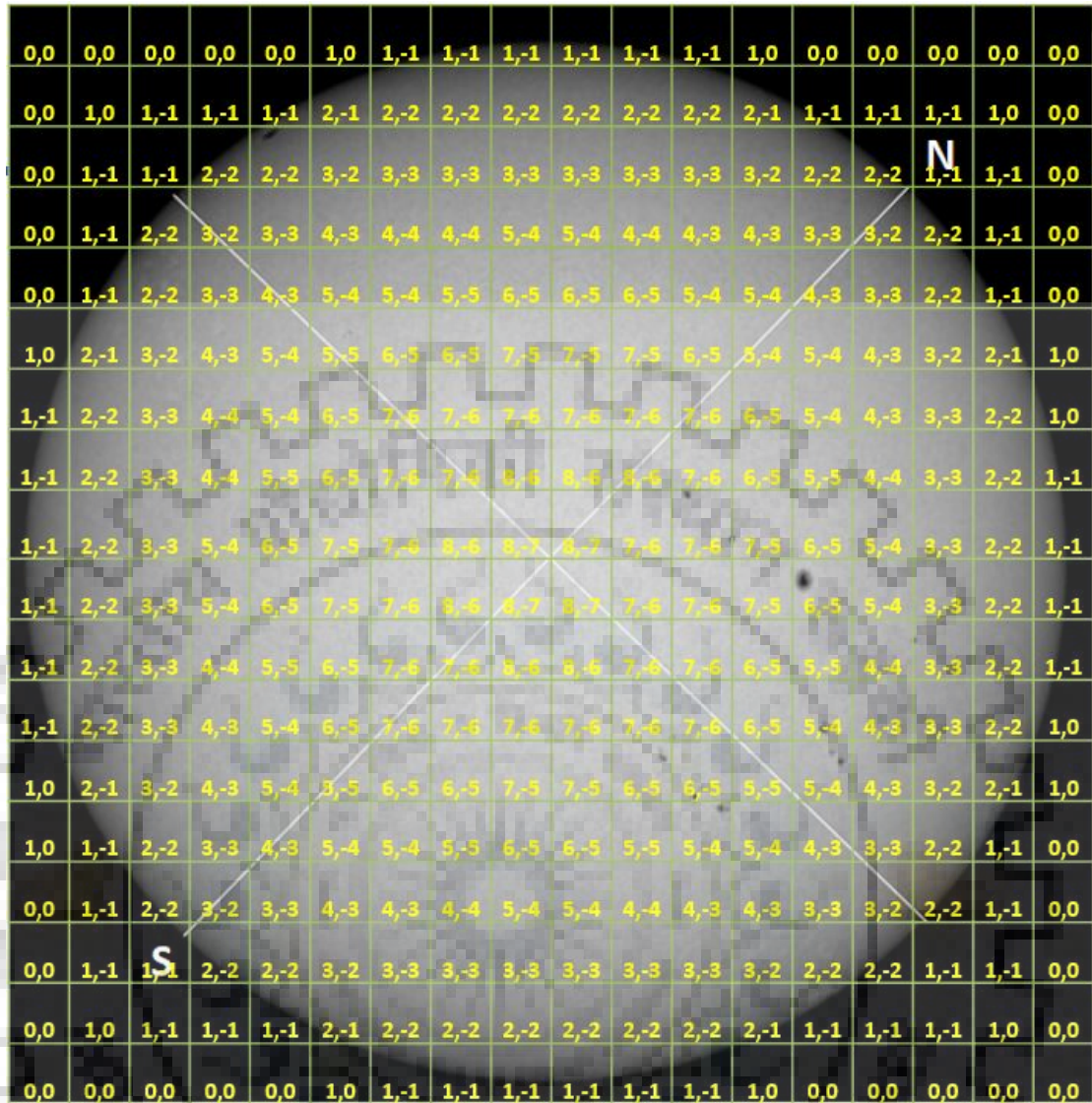


FIGURE 4.6: Pixel Shift along latitude-longitude bands when there is 40° angle between the Solar North and the top of the CCD
Image Courtesy:SDO HMI

Figure 4.9 describes the process for ROI tracking. The user can calculate the shift using formula 2.1 and the pixel coordinates recalculated.

This method uses trigonometric functions like sine and cosine. As discussed earlier, the user can either pre calculate the and cosine functions and upload the values in a look up table or calculate it on-board using Taylor Series expansion. This approach promises good accuracy.

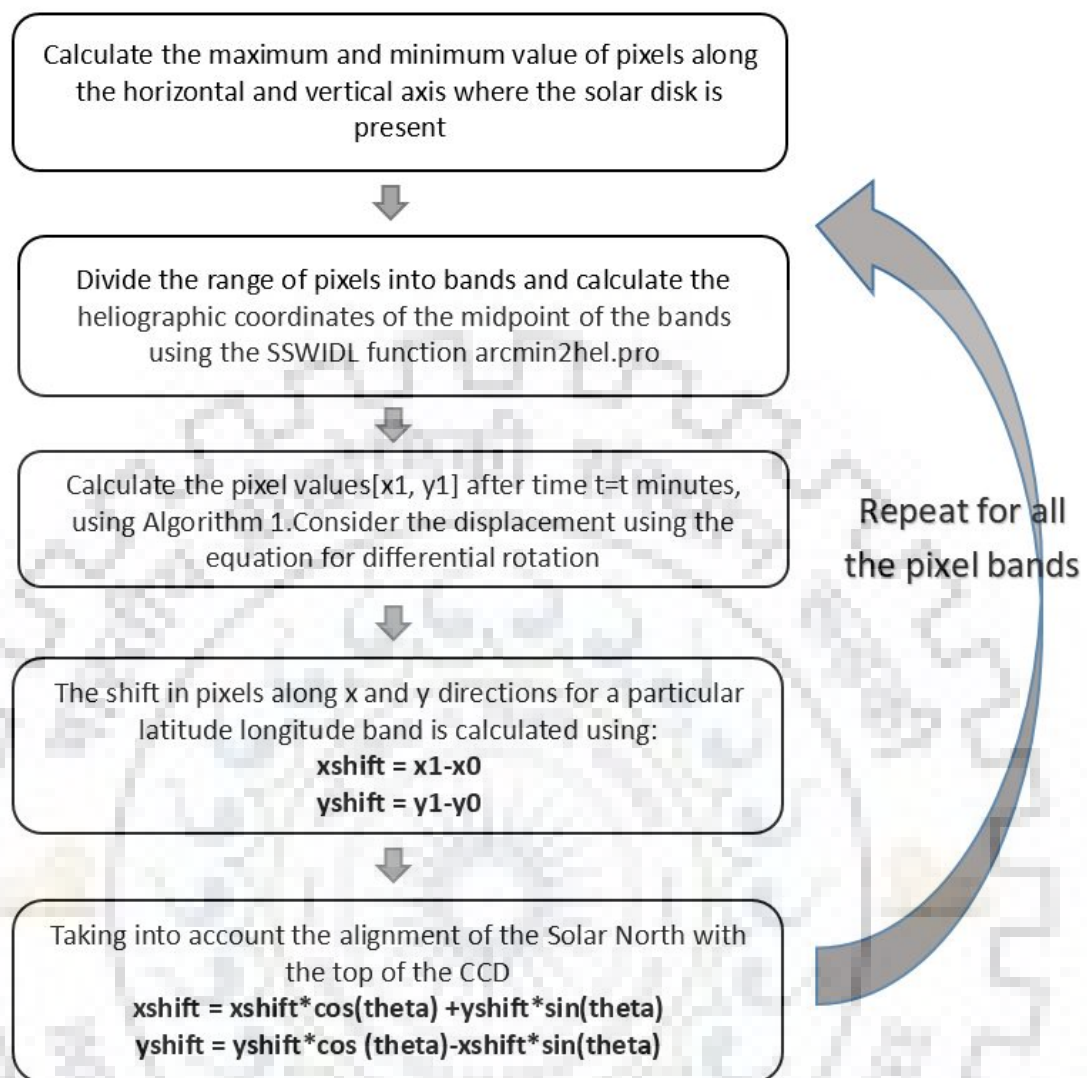


FIGURE 4.7: ROI Tracking: Algorithm 4

4.3 Flare Tracking

Section 3.3 discussed how flare tracking is performed. The methodology of flare tracking is similar to ROI tracking except that the inputs and outputs in flare tracking are in pixel units. The algorithms for flare tracking are derived from the fourth and fifth method for ROI tracking.

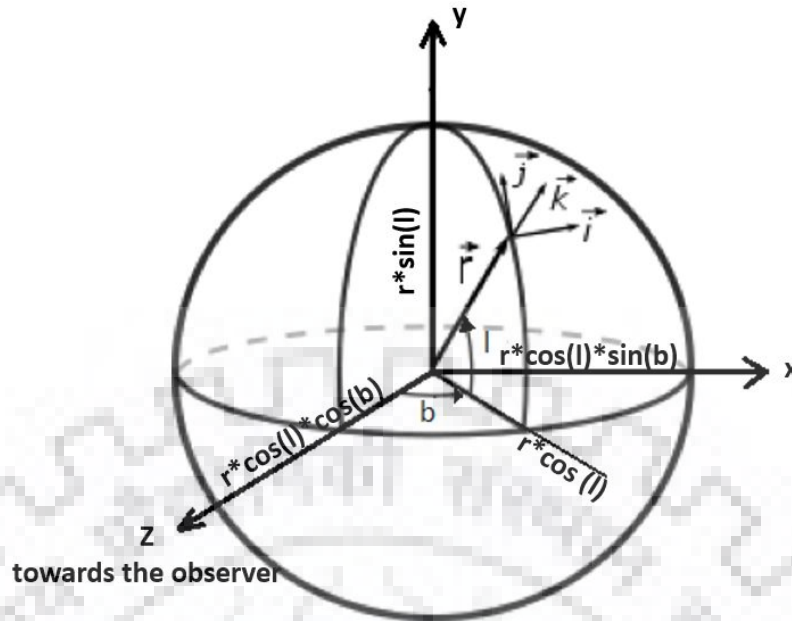


FIGURE 4.8: Spherical to cartesian coordinates Conversion

4.3.1 LUT method

The LUT discussed in section 4.2.4 can also be used for flare tracking. The input pixels are taken from SUIT trigger. As described in figure 4.4, find the value for xshift and yshift from the LUT based on the current pixel position. Jump by 'xshift' and 'yshift' pixels in horizontal and vertical directions respectively. From the central pixels symmetrically calculate the edges of the region under observation. After time t , again fetch the xshift and yshift values from the LUT from its new position and jump accordingly in horizontal and vertical directions. This method saves memory as the same LUT can be used for both ROI tracking and flare tracking.

4.3.2 Flare Cartesian Spherical Coordinate Method

Section 4.2.5 discussed how heliographic coordinates are converted to pixel units by using spherical to cartesian transformation. A step-wise back tracking of the above method is described in figure 4.10 and is proposed for flare tracking.

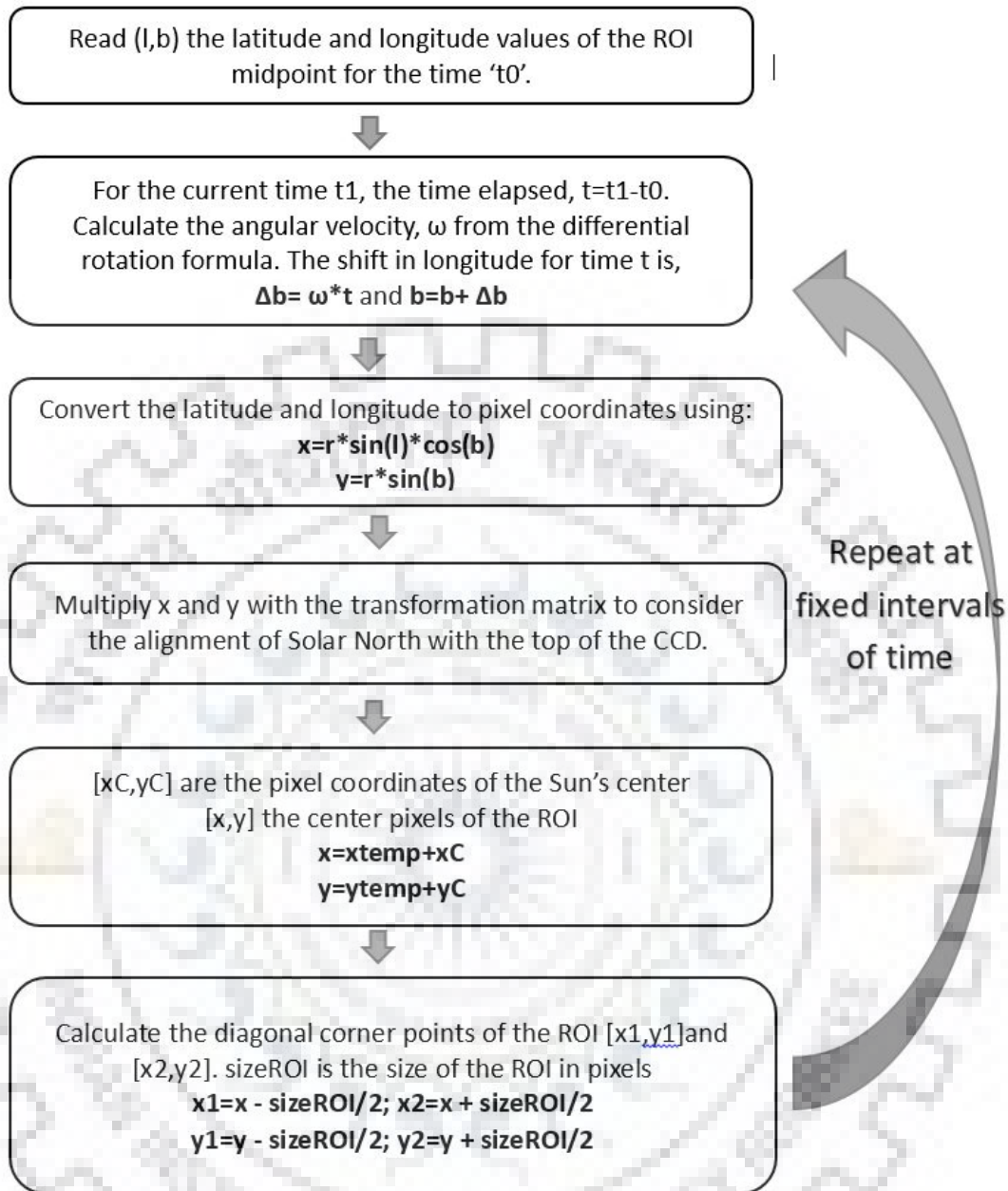


FIGURE 4.9: ROI Tracking: Algorithm 5

The central pixels $[x_C, y_C]$ are removed from the pixel coordinates $[x, y]$. It is multiplied with the inverse of the transformation matrix used in section 4.2.5. The results are converted to arc seconds by multiplying it with the SUIT plate scale and then dividing it by the solar radius (solar radius is in arc seconds). Arc of the 'y' term gives the latitude in radians. The latitude value can then be used to find the longitude using the equations used in Algorithm 5 for ROI tracking.

After time t , find the shift in longitude using the formula 2.1 (latitude value is known) or from the LUT table. The shift is then added to the longitude and the new pixel values are calculated using algorithm 5 discussed in 4.2.5. As we know the values of latitude and longitude, a simple shift along x direction would fetch incorrect results. The ROI Tracking Algorithm 5 takes into account the 'theta' angle. Therefore, in scenarios where theta is not equal to zero the flare region will move both horizontally and vertically. Trigonometric functions like sine, cosine and arc are calculated using Taylor series expansion or using a LUT. The sine and cosine values can be pre-calculated and stored in a LUT.

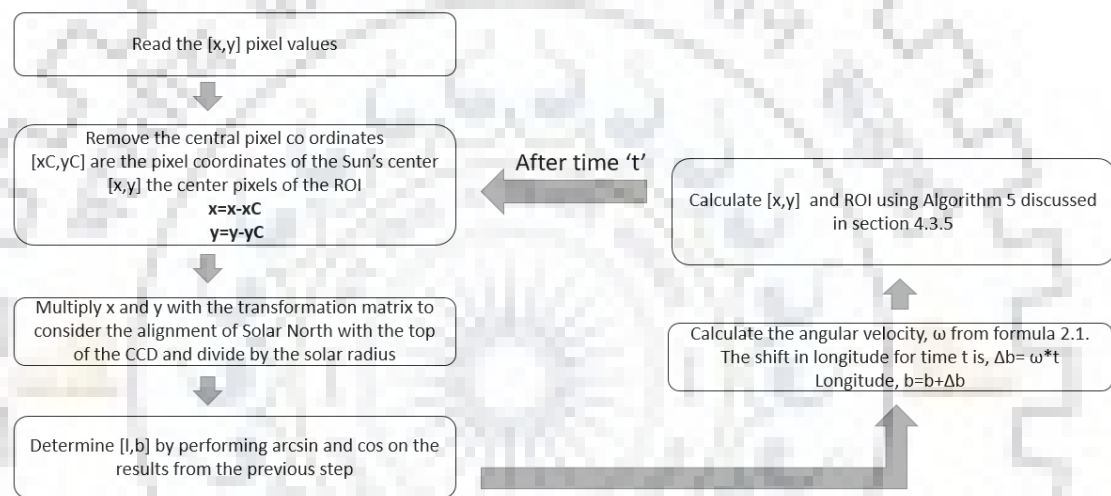


FIGURE 4.10: Flare Tracking: Algorithm 5

Chapter 5

Results and Discussion

Chapter 4 discussed the different approaches to implement ROI and flare tracking. This chapter does a comparative study of the results obtained implementing the ROI tracking and flare tracking algorithms. The error analysis or the deviation from expected values are then calculated and plotted.

5.1 ROI Tracking

For ground based ROI tracking, the user gives heliographic co ordinates of center of the ROI, the angle of inclination of the solar north with respect to the top of the CCD, theta and the duration to observe, t to the SUI data simulator. Figure 5.1 tracks the ROI centered about [40, 30] and theta=0° for a duration of 24 hours. In the top left image, the red box shows the initial position of the ROI. The black box in the images denote the initial position of ROI and the blue box represents the ROI at time intervals of 6 hours, 12hours and 23 hours. A considerable shift in pixels can be observed.

Similarly, figures 5.2 and 5.3 study the ROI about [50,-40] for 24 hours, when the angle of inclination of the solar north with respect to the top of the CCD is 30° and -30° respectively. The red box denotes the initial position of the ROI. The box in blue denotes the ROI a intervals of 6hours, 12hours and 23 hours while

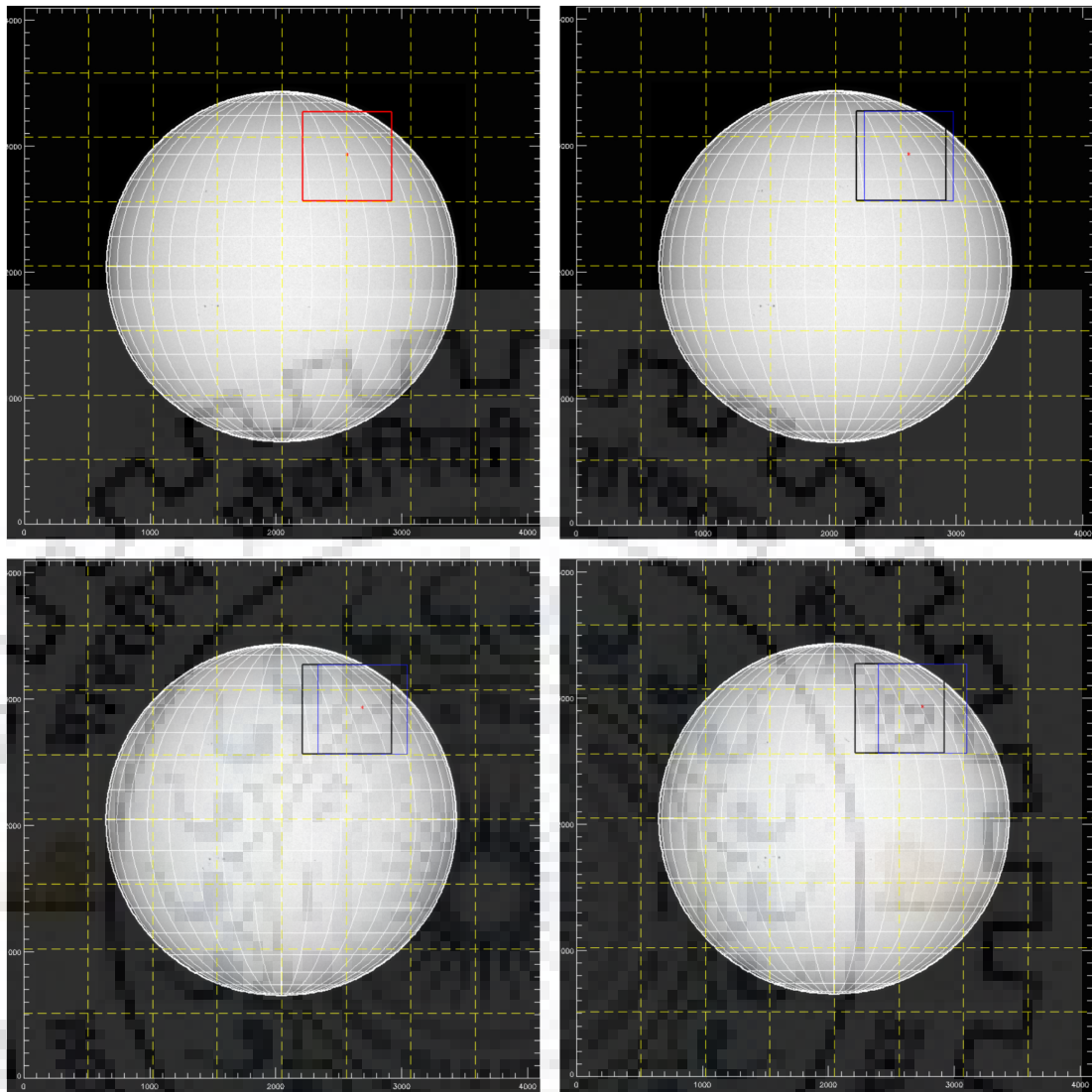


FIGURE 5.1: ROI tracking about $[40,30]$ and $\theta = 0^\circ$ for 24 hours

the black box represents the initial position. It can be seen that when the angle of inclination of the solar north with respect to the top of the CCD, θ is 0° as in figure 5.1 the movement happens only along the x direction. When θ is not equal to 0° as in the case shown in figure 5.3 and 5.2 the shift in pixels happens in both x and y directions.

The size of the ROI in all the above three cases are 704×704 pixels.

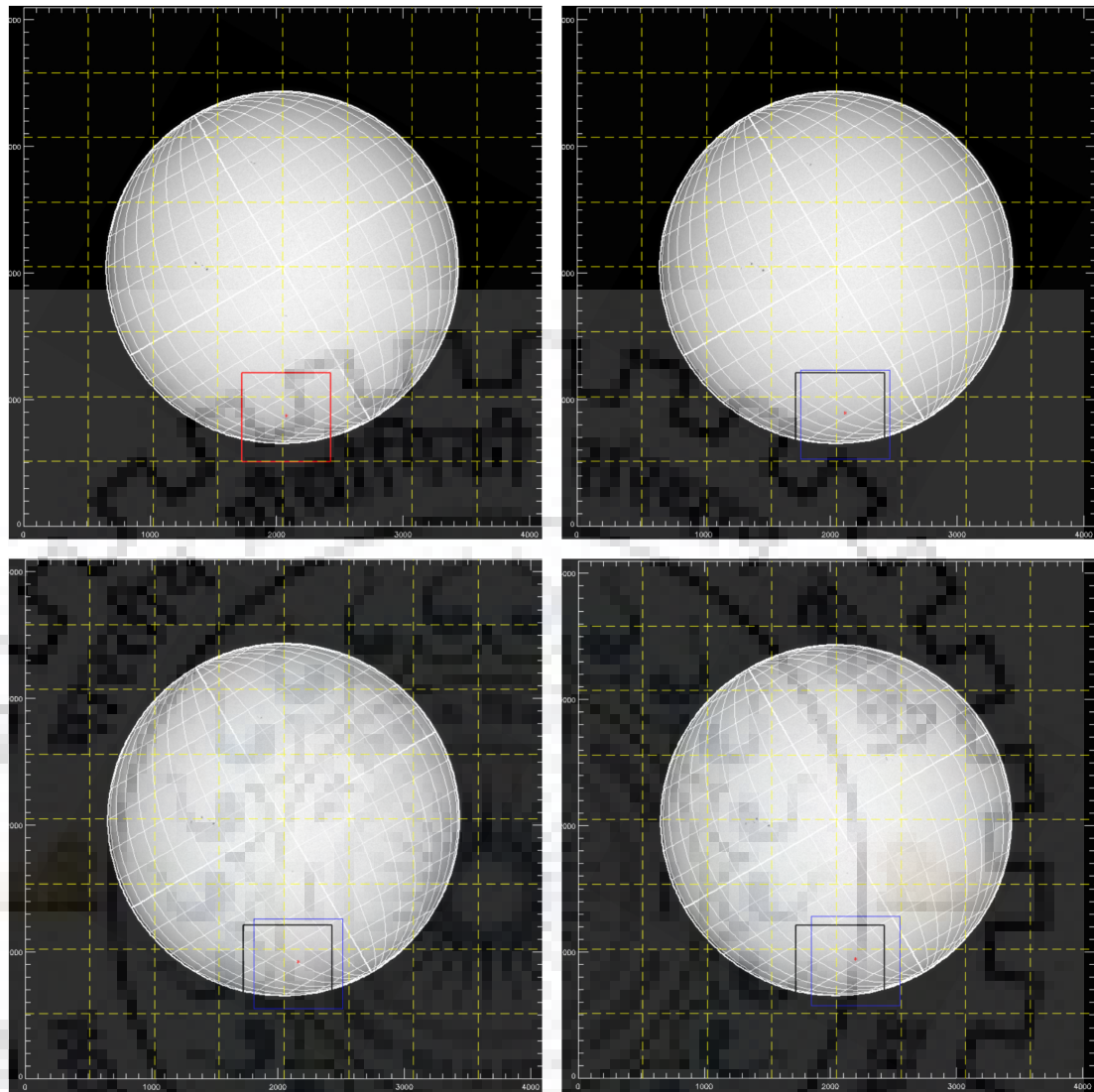


FIGURE 5.2: ROI tracking about $[-50,-40]$ and $\theta = 30^\circ$ for 24 hours

5.2 ROI Algorithms

Chapter 4 discussed five algorithms to implement ROI tracking. Algorithm 1 has 100% accuracy and is being used as reference to study and compare the other four algorithms. Despite its high accuracy its difficult to implement it on an FPGA as it uses trigonometric functions like atan . It can therefore be used by a user at the Payload Operation Centre (POC) to uplink next day's data or to study the received data.

Algorithm 2 has deviation in pixels(with respect to Algorithm 1) of about 300

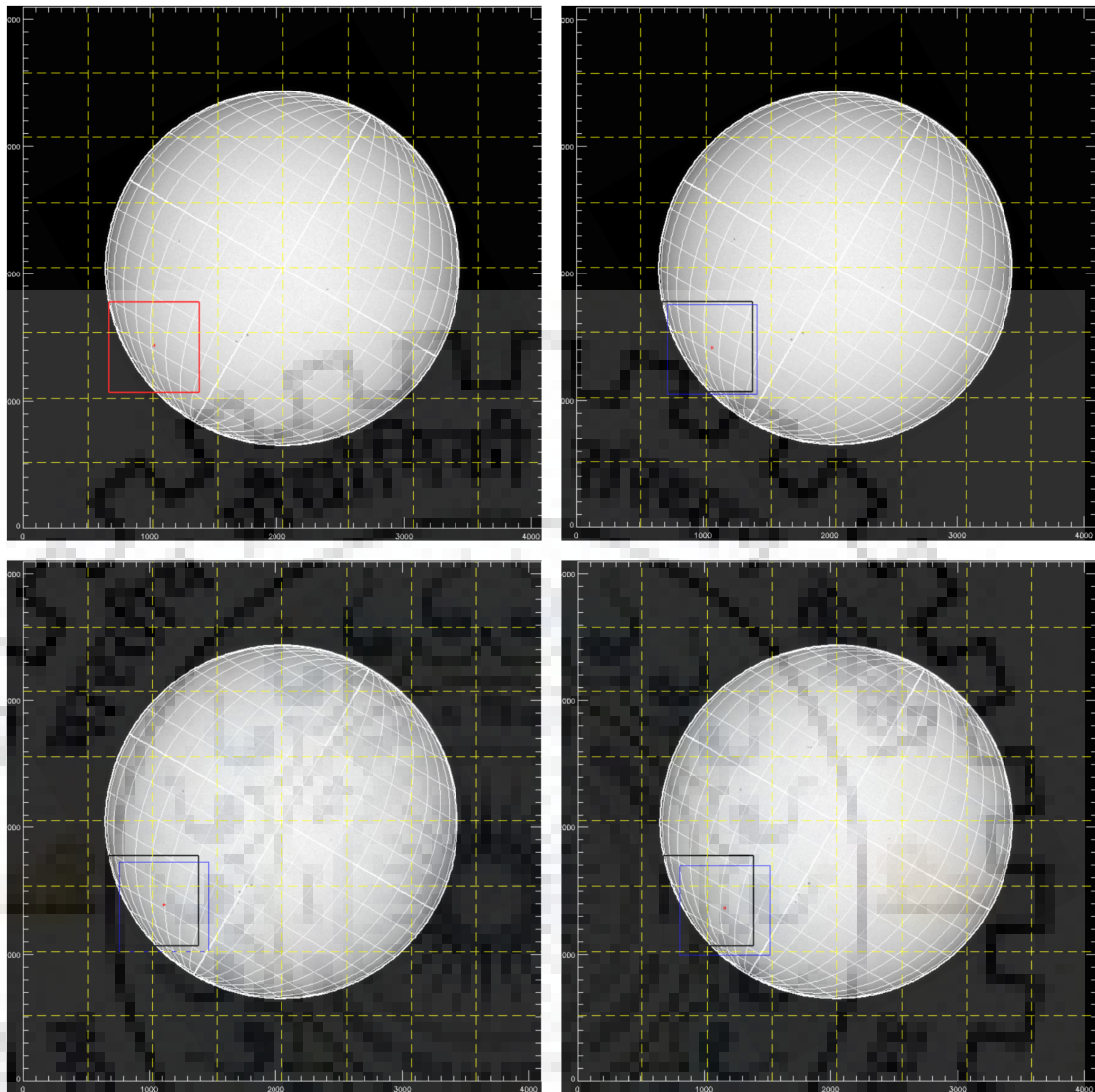


FIGURE 5.3: ROI tracking about $[-50,-40]$ and $\theta = -30^\circ$ for 24 hours

pixels at the poles. It also uses trigonometric functions like sine and cosine which have to be either pre-calculated or calculated using Taylor series.

Based on the input heliographic coordinates, Algorithm 3 fetches the corresponding shift in pixels for that particular 'latitude longitude' band. The onboard computations are simple and easy to implement and the error is significantly lower compared to Algorithm 2.

Algorithm 4 has method of implementation similar to Algorithm 3 the difference being the calculations are here done in pixel units. It has lower error margin compared to Algorithm 3. As the LUT is developed on ground it can be coded

as per requirement and fine tuned to reduce error. Fine tuning includes reducing grid size, better approximations at the limbs. The disadvantage of this method is that the LUT will have to be updated when there is a change in the satellite's position.

With accuracy comparable with Algorithm 1, Algorithm 5 takes into account the P and B0 angles for calculating the pixel values of the input heliographic coordinates. However, when the satellite position changes the transformation matrix(a 2×2 matrix, which takes care of the P,B0) will have to be updated.

Figure 5.4 summarises and does a comparative study of the five ROI algorithms

5.3 Flare Algorithms

As discussed in section 5.2 and 4.2, LUT method and spherical coordinate method have acceptable degrees of accuracy. Hence the two flare tracking algorithms are derived from them.

The LUT method uses the LUT used in ROI tracking (saves memory) to find the shift in pixels with respect to its current position and jump accordingly.

The spherical coordinate for flare tracking uses asine and cosine functions. 0.1 radian is equal to 5.73° . Hence asine function needs a precision of upto two decimal places to resolve the correct latitude value which is then used to calculate the longitude. Hence its suggested to use asine values from a pre calculated LUT.

	Memory Usage	Onboard Calculations	Error Margin
Algorithm 1	Doesnot require much onboard storage space, except for storing the constants like size of ROI, plate scale of the CCD etc.	Uses trigonometric functions like sin,cos, atan etc in calculations which makes it difficult to implement on board.	Very accurate. Used as reference parameter for the other algorithms
Algorithm 2	Doesnot require much onboard storage space, except for storing the constants like size of ROI, plate scale of the CCD etc. A LUT containing the pre calculated values of sin and cos may be used.	Like Algorithm 1, it uses trigonometric functions for calculations. It does not use atan function making it relatively easier to implement if the sin and cos functions are pre calculated and stored onboard. Alternatively, they can be calculated using Taylor series expansion.	Error is minimum at the equatorial regions but becomes significant at the poles
Algorithm 3	Requires memory to store the lookup table. Memory usage would depend on the number of latitude and longitude bands.	Simple addition and subtraction which can be done easily by the FPGA	Relatively low
Algorithm 4	Requires memory to store the lookup table. Memory usage would depend on the pixel size of the bands.	Simple addition and subtraction which can be done easily by the FPGA	Relatively low
Algorithm 5	Requires memory only to store constants like size of ROI, plate scale of the CCD etc. A LUT containing the pre calculated values of sin and cos may be used.	Uses trigonometric functions like sin and cos, which can be either pre calculated or computed onboard using Taylor series expansion.	Accuracy level is good

FIGURE 5.4: Comparative study of the ROI tracking algorithms

5.4 Error Calculation

5.4.1 ROI Tracking

The pixel values are plotted for the range of latitudes for a fixed longitude at varying intervals of time using the proposed ROI tracking algorithms. In figure 5.5, for the fixed longitude of -89° the pixel values are calculated for latitude range from -89° to 89° using the five algorithms and plotted over time period of 2 hours, 6 hours, 12 hours and 23 hours. The graphs on left denote the pixel value along x axis and the graphs on right denote the pixels along y axis.

Longitude=-89

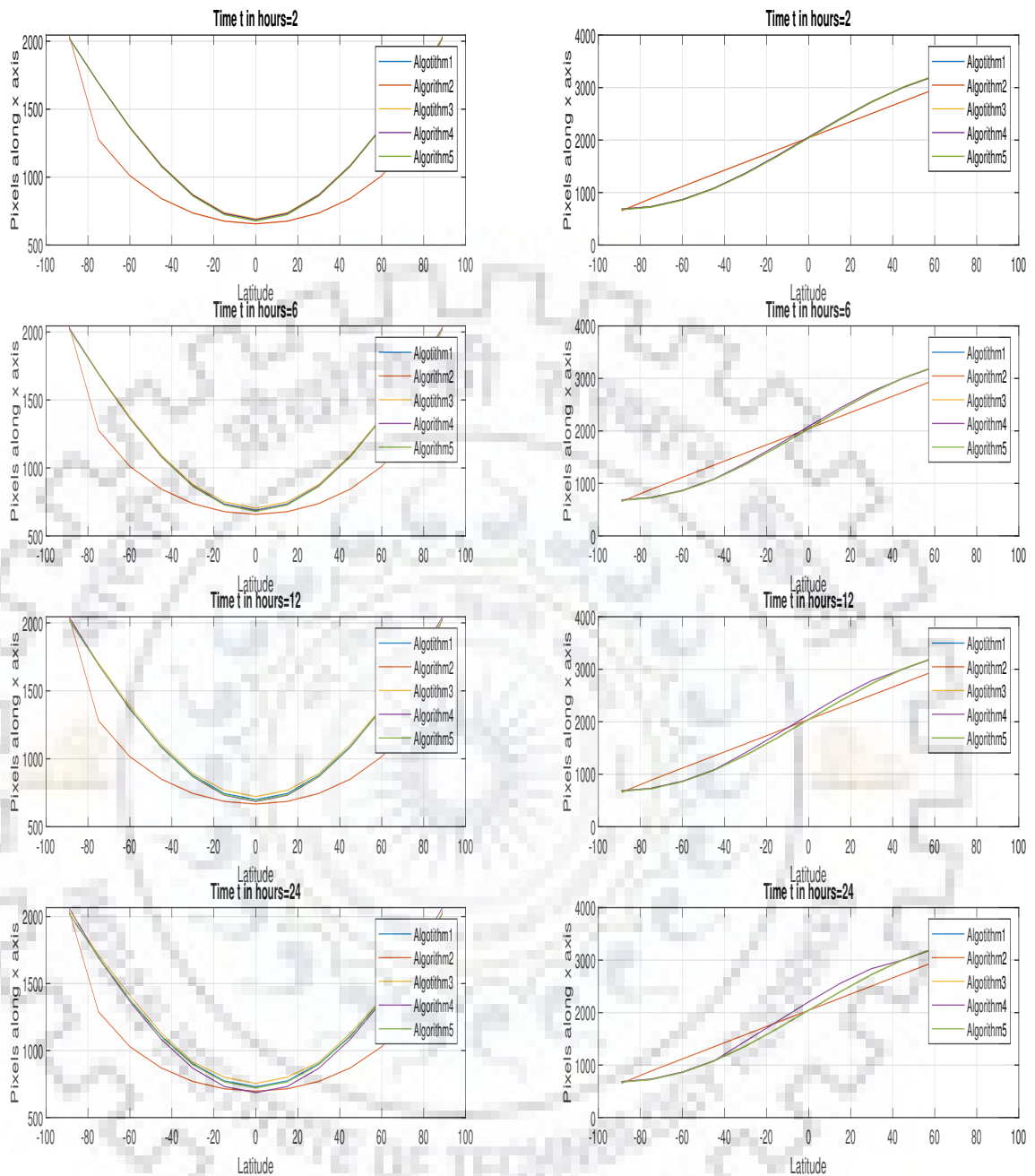


FIGURE 5.5: Study of the pixel position when longitude is -89° over a period of 23 hours

Similar exercise was performed for -45° longitude, 45° longitude and 89° longitude as shown in figure ??, 5.7 and 5.8 respectively.

Longitude=-45

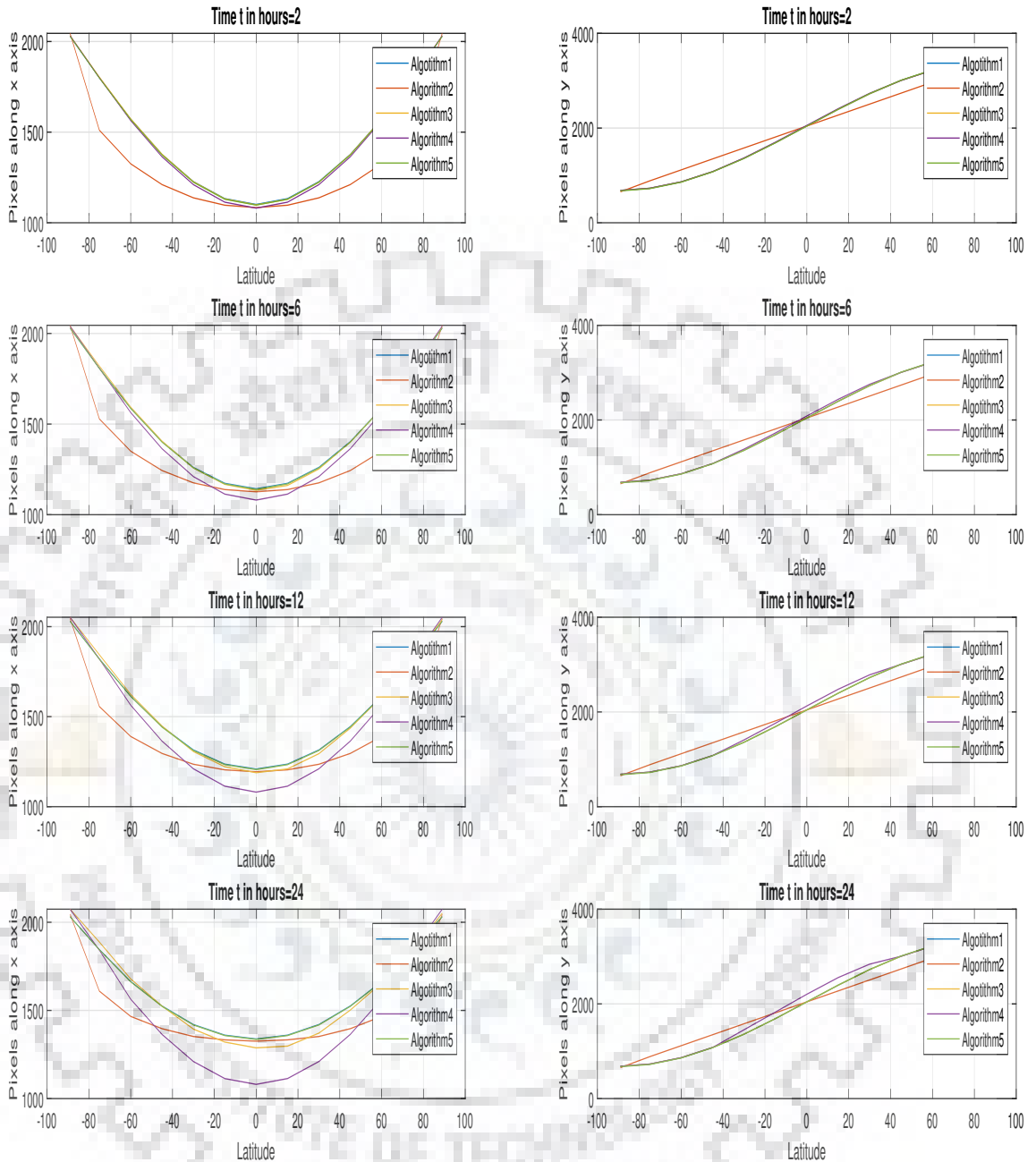


FIGURE 5.6: Study of the pixel position when longitude is -45° over a period of 23 hours

5.4.2 Flare Tracking

Pixel co ordinates for latitude longitude points were calculated. These points were then tracked using the flare tracking algorithms discussed in section 4.3 for a duration of 2 hours, 6 hours, 12 hours and 23 hours. The pixel co ordinates were

Longitude=45

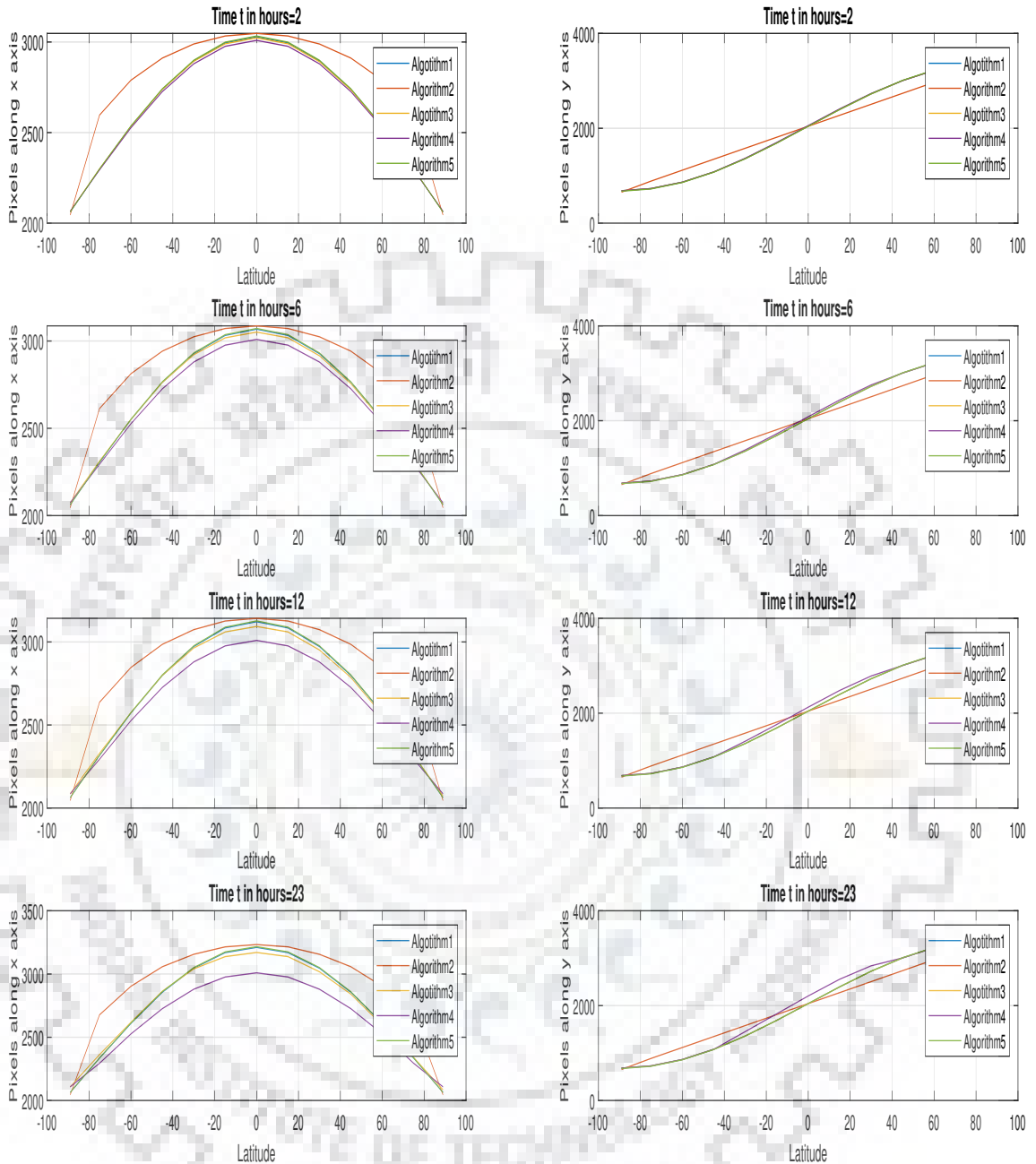


FIGURE 5.7: Study of the pixel position when longitude is -89° over a period of 23 hours

subtracted from the ideal case scenario which was calculated using `hel2arcmin.pro` and `arcmin2hel.pro`. The deviation in pixels is calculated and plotted in figures . For angles greater than 70° their sine values change only at the second decimal. Calculating arcsine using Taylor series does not give precision up to two decimals(

Longitude=89

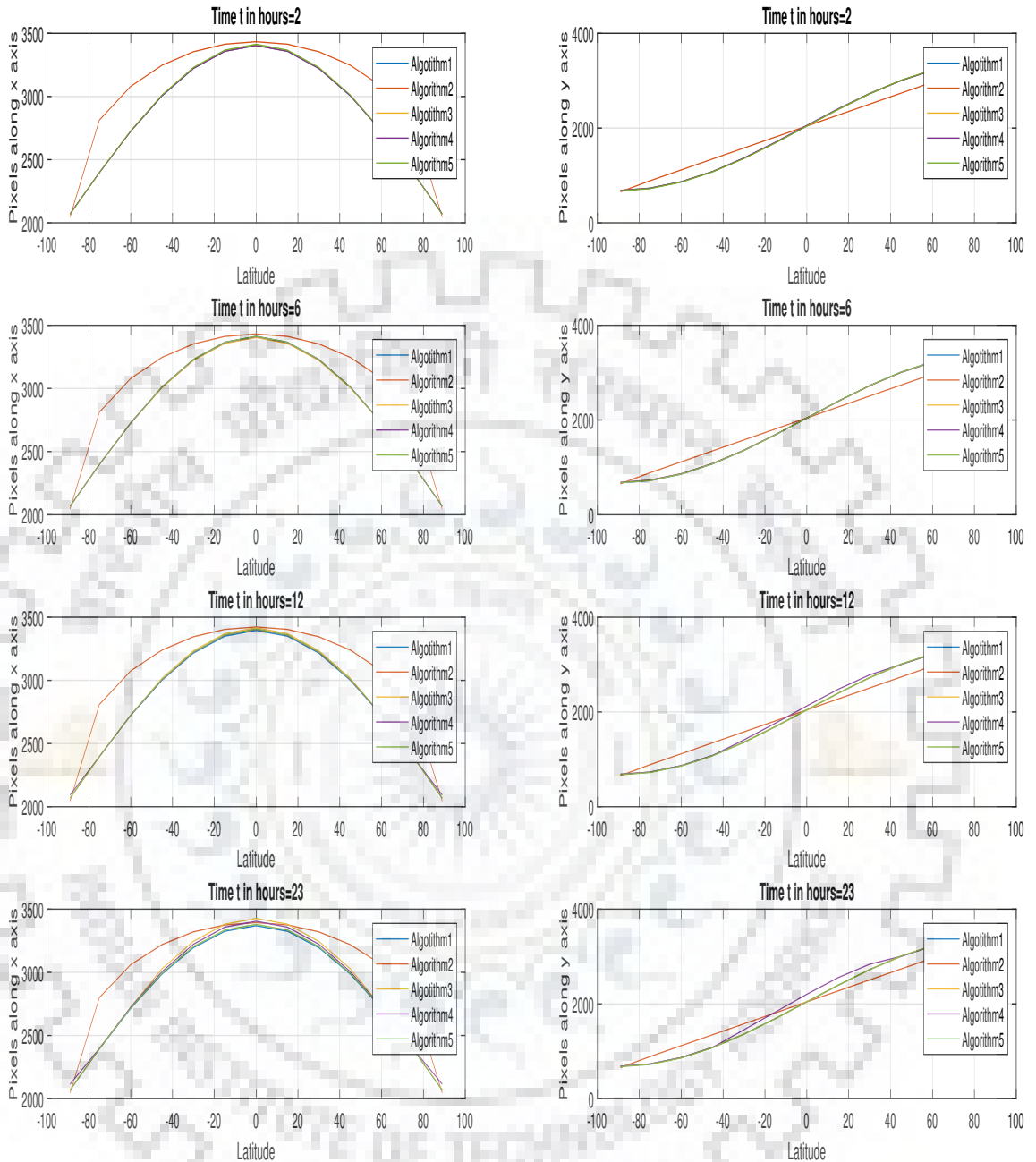


FIGURE 5.8: Study of the pixel position when longitude is 89° over a period of 23 hours

when calculated up to four terms), hence its not useful to use Taylor series expansion for latitudes beyond 70° . Also, when this method was tried for points outside the solar disk it failed.

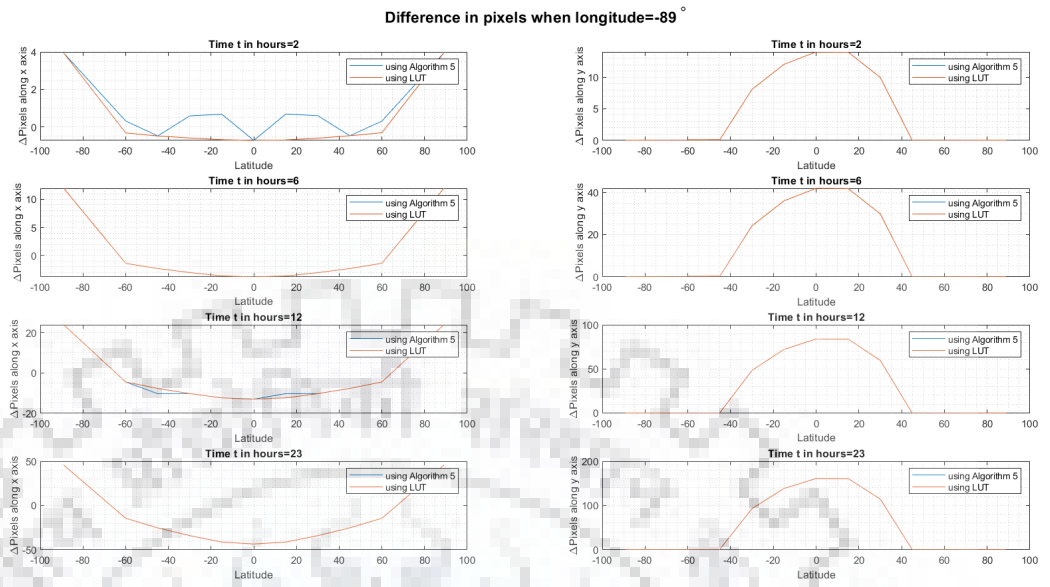


FIGURE 5.9: Study of deviation in pixels from ideal case scenario when longitude= -89° over a period of time

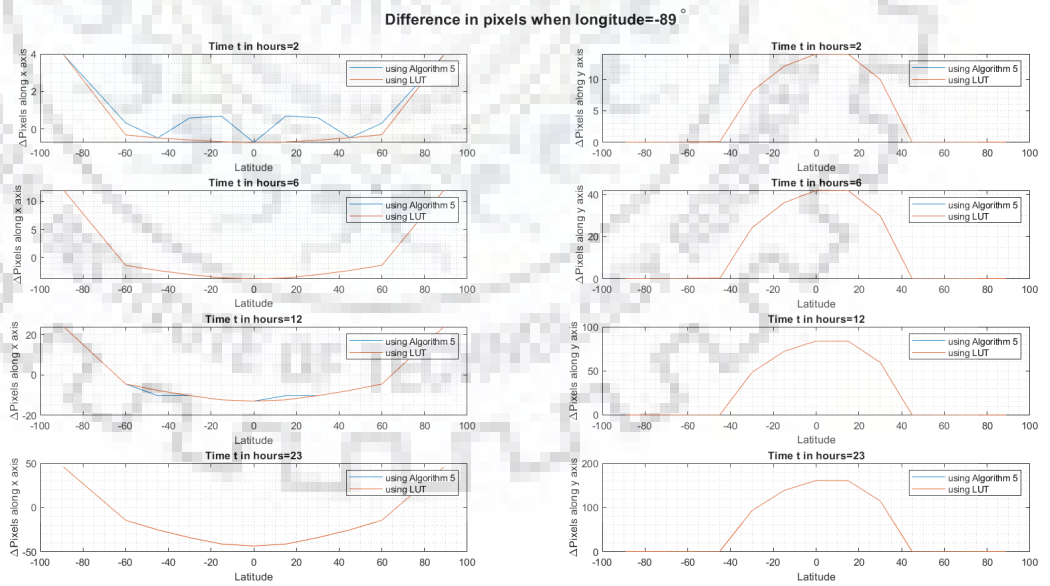


FIGURE 5.10: Study of deviation in pixels from ideal case scenario when longitude= -45° over a period of time

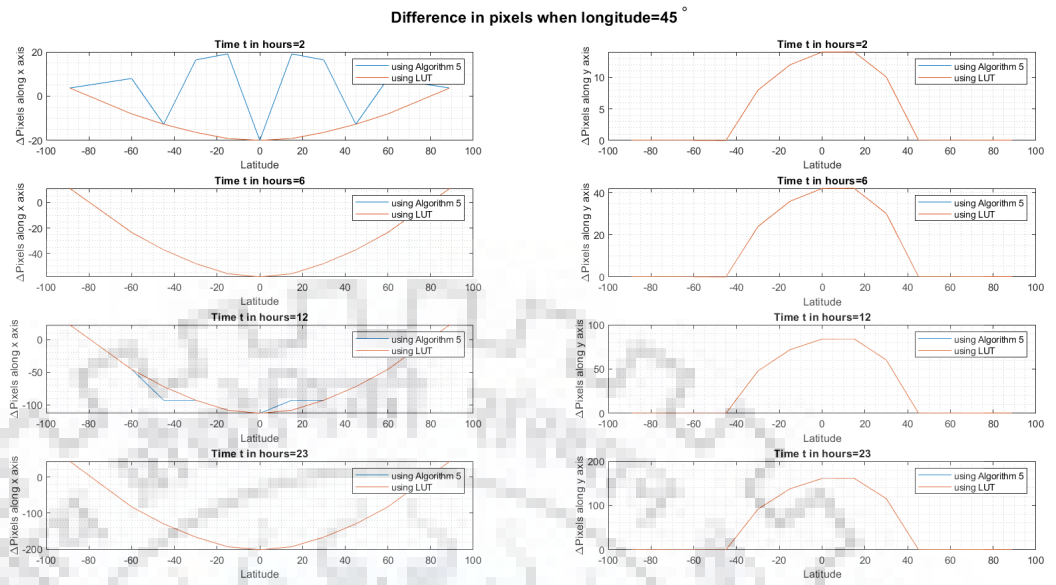


FIGURE 5.11: Study of deviation in pixels from ideal case scenario when longitude= 45° over a period of time

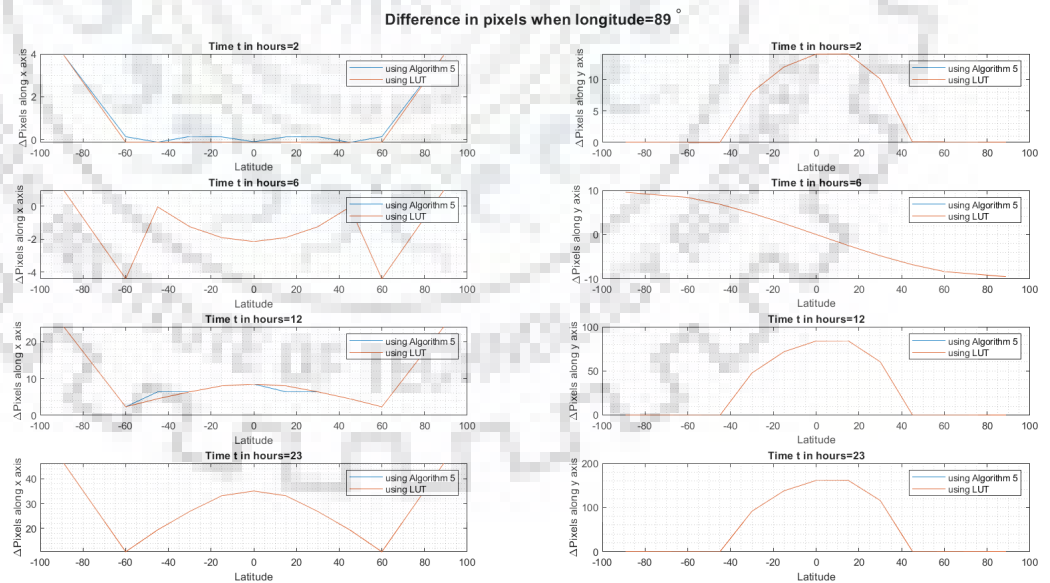


FIGURE 5.12: Study of deviation in pixels from ideal case scenario when longitude= 89° over a period of time

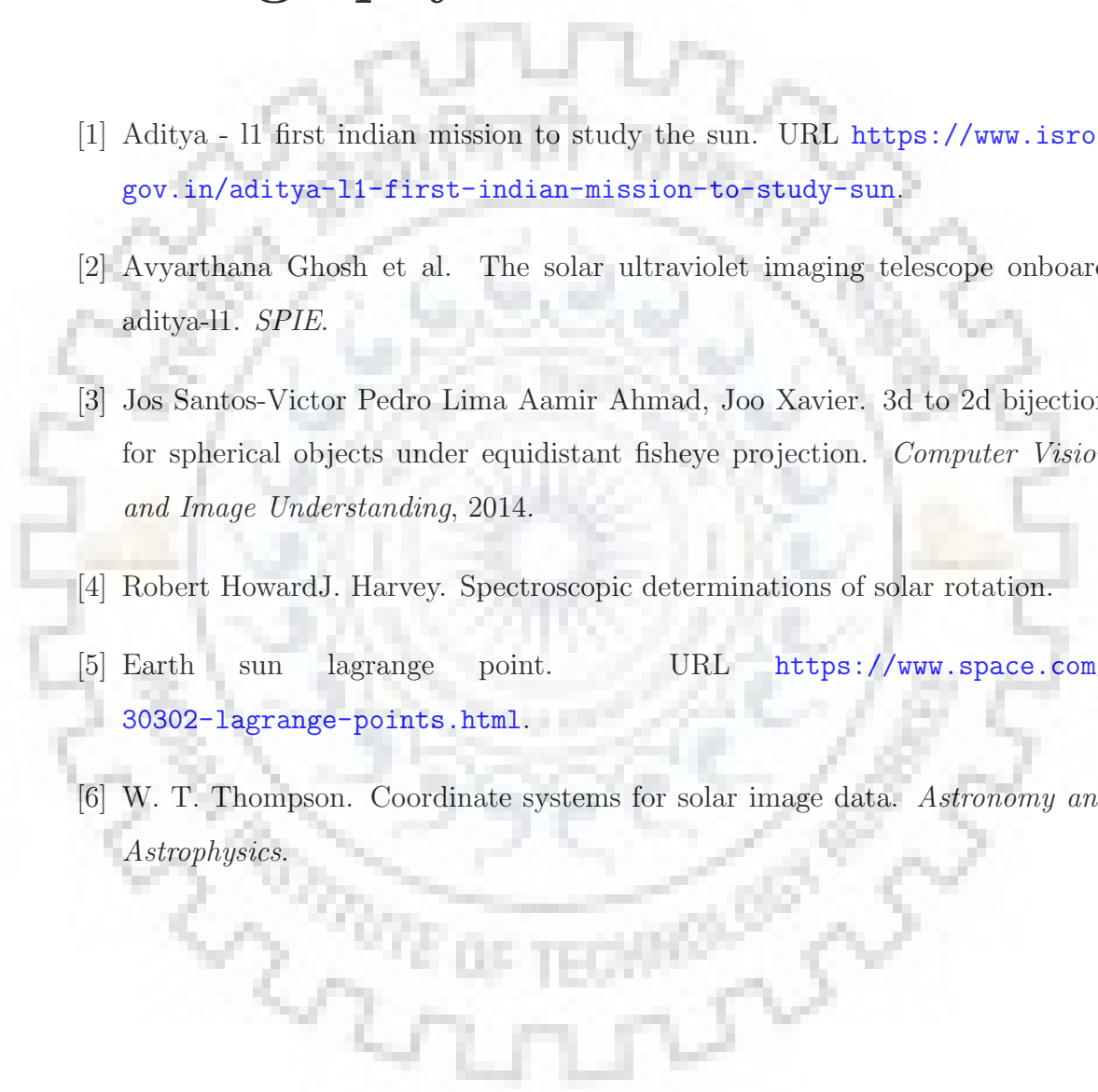
Chapter 6

Summary and Conclusion

For ROI Tracking, Algorithm 1 can be used for ground based calculations. For on board tracking, Algorithm 4 can be used as it is an easy to implement technique on FPGA with relatively low error. It can be reused for flare tracking.

ROI tracking Algorithm 5 can also be implemented if the FPGA can perform trigonometric calculations. A look up table with precalculated values of the trigonometric functions would be required for flare tracking using spherical coordinate method.

Bibliography

- 
- [1] Aditya - 11 first indian mission to study the sun. URL <https://www.isro.gov.in/aditya-11-first-indian-mission-to-study-sun>.
- [2] Avyarthana Ghosh et al. The solar ultraviolet imaging telescope onboard aditya-11. *SPIE*.
- [3] Jos Santos-Victor Pedro Lima Aamir Ahmad, Joo Xavier. 3d to 2d bijection for spherical objects under equidistant fisheye projection. *Computer Vision and Image Understanding*, 2014.
- [4] Robert HowardJ. Harvey. Spectroscopic determinations of solar rotation.
- [5] Earth sun lagrange point. URL <https://www.space.com/30302-lagrange-points.html>.
- [6] W. T. Thompson. Coordinate systems for solar image data. *Astronomy and Astrophysics*.